Platelet Ice under Arctic Pack Ice in Winter

Christian Katlein[1], Volker Mohrholz[2], Igor Sheikin[3], Polona Itkin[4], Dmitry V Divine[4], Julienne Christine Stroeve[5], Arttu Jutila[6], Daniela Krampe[1], Egor Shimanchuk[3], Ian Raphael[7], Benjamin Rabe[1], Ivan Kuznetsov[1], Maria Mallet[1], Hailong Liu[8], Mario Hoppmann[9], Ying-Chih Fang[10], Adela Dumitrascu[11], Stefanie Arndt[1], Philipp Anhaus[1], Marcel Nicolaus[12], Ilkka S. O. Matero[1], and Christian Haas[13]

[1]Alfred-Wegener-Institut Helmholtz-Zentrum für Polar- und Meeresforschung
[2]Institute of Baltic Sea Research Warnemu
[3]Arctic and Antarctic Research Institute
[4]Norwegian Polar Institute
[5]University of Manitoba
[6]Alfred Wegener Institut Helmholtz-Zentrum für Polar- und Meeresforschung
[7]Thayer School of Engineering, Dartmouth College
[8]Shanghai Jiao Tong University
[9]AWI, Germany
[10]Alfred Wegener Institute Helmholtz Centre for Polar and Marine Research
[11]University of Gothenburg
[12]Alfred Wegener Institute
[13]AWI

November 30, 2022

Abstract

The formation of platelet ice is well known to occur under Antarctic sea ice, where sub-ice platelet layers form from supercooled ice shelf water. In the Arctic however, platelet ice formation has not been extensively observed and its formation and morphology currently remain enigmatic. Here, we present the first comprehensive, long-term in situ observations of a decimeter thick sub-ice platelet layer under free-drifting pack ice of the Central Arctic in winter. Observations carried out with a remotely operated underwater vehicle (ROV) during the midwinter leg of the MOSAiC drift expedition, provide clear evidence of the growth of platelet ice layers from supercooled water present in the ocean mixed layer. This platelet formation takes place under all ice types present during the surveys. Oceanographic data from autonomous observing platforms lead us to the conclusion that platelet ice formation is a widespread but yet overlooked feature of Arctic winter sea ice growth.

Platelet Ice under Arctic Pack Ice in Winter

Christian Katlein[1]*, Volker Mohrholz[2], Igor Sheikin[3], Polona Itkin[4], Dmitry V. Divine[5], Julienne Stroeve[6,7], Arttu Jutila[1], Daniela Krampe[1], Egor Shimanchuk[3], Ian Raphael[8], Benjamin Rabe[1], Ivan Kuznetov[1], Maria Mallet[1], Hailong Liu[9], Mario Hoppmann[1], Ying-Chih Fang[1], Adela Dumitrascu[10], Stefanie Arndt[1], Philipp Anhaus[1], Marcel Nicolaus[1], Ilkka Matero[1], Marc Oggier[11], Hajo Eicken[11], Christian Haas[1]

[1]Alfred-Wegener-Institut Helmholtz-Zentrum für Polar- und Meeresforschung, Bremerhaven, Germany

[2] Leibniz Institute for Baltic Sea Research, Rostock-Warnemünde, Germany

[3]Arctic and Antarctic Research Institute, St.Petersburg, Russia

[4]UiT University of Tromsø, Tromsø, Norway

[5]Norwegian Polar Institute, Tromsø, Norway

[6]University College of London, London, United Kingdom

[7]Center for Earth Observation Science, Department of Environment & Geography, University of Manitoba, Winnipeg, MB, Canada

[8]Thayer School of Engineering, Dartmouth College, Hanover NH, United States of America

[9]Shanghai Jiao Tong University, Shanghai, China

[10]University of Gothenburg, Gothenburg, Sweden

[11]International Arctic Research Center, University of Alaska Fairbanks, Fairbanks AK, United States of America

*Corresponding author: Christian Katlein (ckatlein@awi.de)

Key Points:

- Extensive observation of platelet ice formation under Arctic winter sea ice
- The sub-ice platelet layer appears to form locally due to seed crystals in ocean surface supercooling.

Word count = 4500 words

Abstract

The formation of platelet ice is well known to occur under Antarctic sea ice, where sub-ice platelet layers form from supercooled ice shelf water. In the Arctic however, platelet ice formation has not been extensively observed and its formation and morphology currently remain enigmatic. Here, we present the first comprehensive, long-term in situ observations of a decimeter thick sub-ice platelet layer under free-drifting pack ice of the Central Arctic in winter. Observations carried out with a remotely operated underwater vehicle (ROV) during the midwinter leg of the MOSAiC drift expedition, provide clear evidence of the growth of platelet ice layers from supercooled water present in the ocean mixed layer. This platelet formation takes place under all ice types present during the surveys. Oceanographic data from autonomous observing platforms lead us to the conclusion that platelet ice formation is a widespread but yet overlooked feature of Arctic winter sea ice growth.

Plain language summary

Platelet ice is a particular type of ice that consists of decimeter sized thin ice plates that grow and collect on the underside of sea ice. It is most often related to Antarctic ice shelves and forms from supercooled water with a temperature below the local freezing point. Here we present the first comprehensive observation of platelet ice formation in freely drifting pack ice in the Arctic in winter during the international drift expedition MOSAiC. We investigate its occurrence under the ice with a remotely controlled under-ice diving robot. Measurements of water temperature from automatic measurement devices distributed around the central MOSAiC ice floe show, that supercooled water and thus platelet ice occurs widely in the winter Arctic. This way of ice formation in the Arctic has been overlooked during the last century, as direct observations under winter sea ice were not available and contrary to typical Antarctic observations, manifestation of platelet ice in Arctic ice core stratigraphy has been more challenging to identify.

1. Introduction

Platelet ice is a characteristic feature of Antarctic landfast sea ice, where supercooled ice shelf waters lead to the advection and growth of sub-ice platelet layers [*Hoppmann et al.*, 2020]. They consist of loosely attached decimeter sized plate-shaped ice crystals [*Hoppmann et al.*, 2017; *Langhorne et al.*, 2015; *Smith et al.*, 2001] and can be up to several meters thick. These ice platelets form by nucleation in supercooled layers of seawater either at depth [*Dieckmann et al.*, 1986] or directly at the ice underside [*Leonard et al.*, 2006; *Mahoney et al.*, 2011] in the vicinity of large ice shelves, which provide supercooled water due to basal ice shelf melt in the water circulation of ice shelf cavities. The porous structure provides shelter for a particular ice associated ecosystem [*Arrigo et al.*, 2010; *Günther and Dieckmann*, 2004; *Vacchi et al.*, 2012] and is thus important for biogeochemical cycles [*Thomas and Dieckmann*, 2002].

As ice shelves are much less common in the Arctic [*Dowdeswell and Jeffries*, 2017], observations of platelet ice in the Arctic are rare and the processes causing its formation are poorly understood. The availability of supercooled water plays a central role for the growth of decimeter scale ice platelets [*Lewis and Perkin*, 1983; 1986; *Weeks and Ackley*, 1986]. *Jeffries et al.* [1995] presented one of the few descriptions of platelet ice in the Arctic Ocean. Their study identified platelet ice crystals in 22 out of 57 ice cores collected in the Beaufort Sea during August and September 1992 and 1993. They suggest four different sources for supercooled water, two of which require the presence of ice shelves and coastal interactions and are therefore not relevant for the central Arctic Ocean. The other two include small scale “ice pump” mechanisms [*Lewis and Perkin*, 1983; 1986] and the interaction of summer meltwater with the underlying colder seawater, leading to the formation of false bottoms in under-ice melt ponds and platelet ice crystals [*Eicken*, 1994; *Martin and Kauffman*, 2006; *Notz et al.*, 2003]. They describe platelet ice as a widespread feature in the Beaufort Sea based on their ice-core analysis. *Carnat et al.* [2017] describe two cores with platelet ice signature. Early observations from *Lewis and Lake* [1971] stay vague in the description, but show that the phenomenon is not new. The Russian drifting station NP-2015 also detected platelet formation caused by meltwater percolation through the ice cover (personal communication I. Sheikin) and an indirect observation under fast ice in summer was described by *Kirillov et al.* [2018].

Sub-ice platelet layers can be separated from frazil ice in such way that the geometric size of the platelet ice crystals is on the order of 1-10 cm. Frazil ice describes the crystal habit resulting from the initial stages of sea-ice growth, when small disk and needle-like crystals smaller than 1 cm appear suspended in the upper water column or at the ocean surface [*Hoppmann et al.*, 2020; *Weeks and Ackley*, 1986; *Zubov*, 1963]. Sub-ice platelet layers exhibit a rather random orientation of crystal axes. This is significantly different from the skeletal layer at the bottom of growing sea ice, where parallel oriented ice lamellae are growing into a microscale layer of constitutionally supercooled water caused by the brine expulsion during sea-water freezing [*Lofgren and Weeks*, 2017; *Rutter and Chalmers*, 1953; *Shokr and Sinha*, 2015].

No extensive direct in situ observations of platelet ice under Arctic sea ice particularly during winter are available. Anecdotal reports from divers, such as during the Tara expedition [*Ragobert et al.*, 2008] or the "Under the Pole" diving expedition [*Bardout et al.*, 2011], allude that this feature has been mostly overlooked in the Central Arctic. Figure S1 and Table ST1 provide an overview of previous observations.

Here, we present the first extensive, more systematic in situ observations of growing sub-ice platelet layers under Arctic sea ice in winter. Dives with a remotely operated vehicle during the international Arctic drift expedition "Multidisciplinary Observatory for the Study of Arctic Climate" (MOSAiC) from January to March 2020 around 88°N (Figure 1) revealed a widespread coverage of decimeter scale platelet ice crystals growing on and under the bottom of the ice.

2. Materials and Methods

2.1 Study Area

The ice floe of the MOSAiC drift experiment of the German research icebreaker Polarstern [*Knust*, 2017] consisted of a conglomerate of various ice types, out of which deformed second year ice and relatively level residual ice (first year ice grown into a remaining matrix of very rotten melted ice [*WMO*, 2014]) were the most abundant. Initial ice thicknesses during the mobilization of the drift station in the beginning of October 2019 were as little as 20-30 cm for the residual ice and around 60-80 cm for the undeformed second year ice [*Krumpen et al.*, 2020]. By March, ice growth had increased the level ice thickness to about 145 cm for the residual ice and around 200 cm for the second year ice (Figure S2). Pressure ridges with typical keel drafts of 5-7 m and maximum of 11 m characterized the deformed ice. More details about the composition and history of the MOSAiC floe can be found in *Krumpen et al.* [2020].

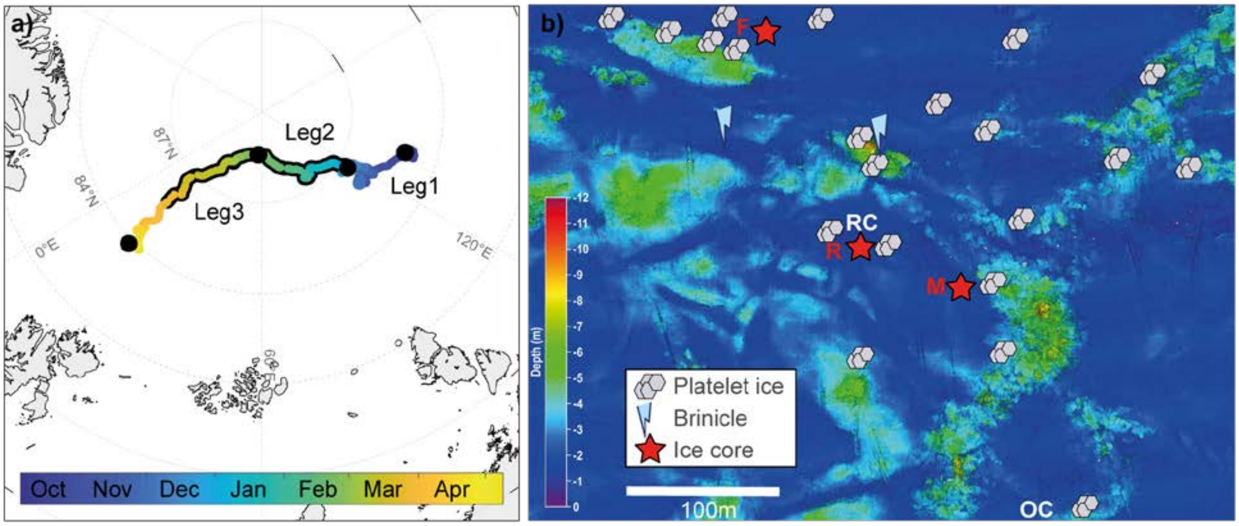

Figure 1. a) Drift track of MOSAiC floe in the Central Arctic Ocean from October 2019 to mid-May 2020. Black dots denote start and end of drift legs 1, 2 and 3, respectively. Platelet ice was observed between 30 December 2019 and 28 March 2020 (black highlighted track). b) Map of ice draft derived from multibeam sonar survey on 21 January 2020 with most prominent locations of the ubiquitous platelet ice observations (grey symbols), brinicles (light blue symbols) and ice core samples (red stars). White letters indicate the position of the ROV access hole (RC) and the MSS deployment hole (OC). Red letters refer to ice cores taken at the ROV site (R), the ice mechanics site (M) and the ridge site (F).

2.2 ROV Operations

We carried out remotely operated vehicle (ROV) dives from a hole through the ice covered by a heated tent. The M500 ROV (Ocean Modules, Atvidaberg, Sweden) was equipped with a comprehensive sensor suite including cameras as well as a 240 kHz multibeam sonar [*Katlein et al.*, 2017] and provided an operating range of 300 m from the access hole. We documented platelet ice occurrences mostly with four cameras: a high definition zoom video camera (Surveyor HD, Teledyne Bowtech, Aberdeen, UK), two standard definition video cameras (L3C-720, Teledyne Bowtech, Aberdeen, UK) and a 12 megapixel still camera (Tiger Shark, Imenco AS, Haugesund, Norway).

The ROV dives covered many different sites, but several places were revisited (Figure 1b) due to repeating routine dive missions allowing for a temporal assessment of platelet ice evolution. On 15 February 2020, we towed an under-ice zooplankton net (ROVnet) with the ROV directly along the ice underside [*Wollenburg et al.*, 2020] to brush off platelet ice samples for structural analysis. In the lab, platelets were frozen into a solid block of ice by adding sea water to the sample container, in order to later analyze the platelet ice crystal structure.

2.3 Ice Core Sampling and Analysis

We extracted ice cores in three locations (Figure 1b) where sub-ice platelet coverage had been previously confirmed by ROV imagery. We analyzed them for ice texture by preparing thin sections using the Double Microtoming Technique [*Eicken and Salganek*, 2010; *Shokr and Sinha*, 2015] in the lab on board. We photographed the thin sections between crossed polarizers to identify crystal geometric properties. To associate an approximate date of ice formation to each ice sample along the core, we used a simple ice-growth model based on the number of freezing-degree-days [*Pfirman et al.*, 2004], forced by air temperatures recorded by the Polarstern weather station.

2.4 Physical Oceanographic Measurements

We measured vertical and horizontal profiles of seawater conductivity, temperature, and pressure (CTD) using three independent different types of platforms. One CTD sensor was mounted on the ROV (GPCTD, SeaBird Scientific, USA), while we performed recurring deployments of a free-falling microstructure sonde (MSS 90LM, Sea and Sun Technologies, Trappenkamp, Germany) through a nearby hole in the ice (Figure 1b). In addition, several autonomous stations with CTD packages at a depth of 10 m (SBE37, SeaBird Scientific, USA) were operational in the MOSAiC distributed network at distances of 10-40 km from the central floe (Figure S3). All devices were calibrated by the manufacturers immediately before the expedition. The respective measurement uncertainties are discussed in supplementary text T1.

3. Results and Discussion

3.1 Sub-ice Platelet Layer Morphology

We observed a 5 to 30 cm thick sub-ice platelet layer covering the ice bottom as shown in Figure 2. The ice platelets are composed of blade- or disc-shaped single ice crystals with c-axis alignment normal to the platelet surface. Most platelets were firmly attached to their substrate but fragile to physical impact by the ROV. When observed on ropes or chains, platelet ice crystals were tightly grown through their structure (Figures 2b, S4) and not just loosely attached to the respective surface. This indicates that these platelets grew on site and have not been advected in from deeper waters or horizontally as already suggested by *Lewis and Lake* [1971]. Contrary to Antarctic fast ice, we did not find meter thick layers of platelet ice accumulation [*Hoppmann et al.*, 2017; *Hunkeler et al.*, 2016], possibly due to slower platelet or faster congelation growth. The freezing front of the congelation ice quickly progressed downward into the sub-ice platelet layer and incorporated it by congelation ice growth in between the platelet crystals [*Dempsey et al.*, 2010]. A thickness difference between Arctic and Antarctic sub-ice platelet layers was already proposed by *Lewis and Perkin* [1986] based on different driving depths in the ice pump mechanism.

We identified crystal sizes up to approximately 15 cm from the ROV camera footage. Maximum crystal size retrieved with the towed zooplankton net was 9 cm, while the thicknesses of platelet crystals ranged from 0.8-2.5 mm. However, due to the limited size of the sampling bottle with a diameter of 10 cm and the physical interaction of the ROVnet (0.4 by 0.6 m opening) and platelet ice structures, platelets may well have been broken during the sampling process.

Platelet ice growth depends on available crystallization nuclei or seed crystals for secondary nucleation. Probably due to this reason, we did not observe platelet growth on the polymer-covered thermistor strings hanging in the water column. The complex structure of core-mantle polyamide rope or metal parts provided sufficient crystallization nuclei for platelet formation (Figures 2d, S4). Another explanation could be material dependent adhesion of seed crystals as described in *Robinson et al.* [2020]. This was particularly obvious on 15 February 2020, when the ROV had been hanging for three days in 2 m water depth and was covered in up to 30 mm large platelet crystals on edges and corners, while particularly smooth plastic surfaces were unaffected by platelet growth (Figure S5).

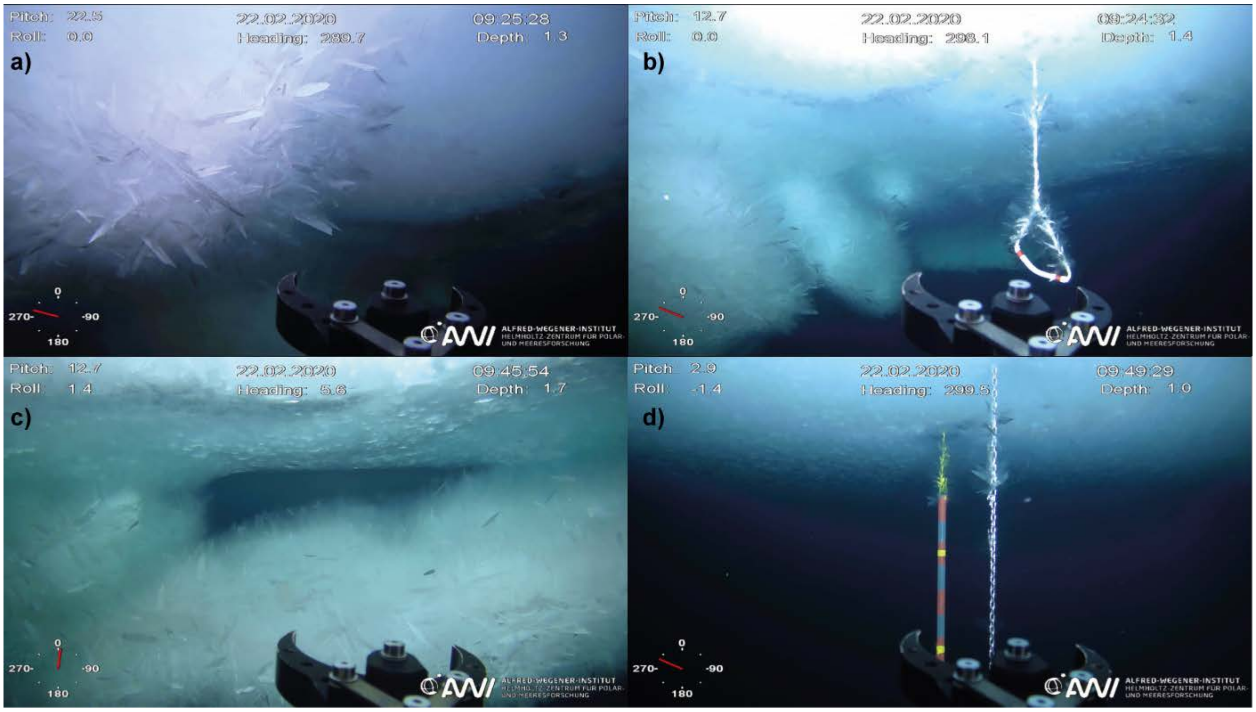

Figure 2. a) Close-up picture of platelet ice covering a ridge block. The ROV manipulator opening in the foreground is about 9 cm wide. b) Rope sling next to a pressure ridge: both, the rope and the ridge are vastly covered in ice platelets. c) Upward growing platelet ice in a ridge cavity. d) Platelet ice crystals covering the rope and chain of underwater installations. Note the lack of platelet growth on the plastic marker stick and the coverage of small platelet crystals underneath the level ice.

3.2 Spatial Distribution of Platelets

Platelet ice coverage was ubiquitous in the entire observational range of the ROV. However, platelet ice growth was almost exclusively observed in the uppermost part of the water column, above a depth of 2-3 m. Deeper lying ridge keels as well as deep hanging ropes and instrument installations were not covered in platelet ice. Few installations exhibited a vertical gradient of platelet ice growth coverage, with the most extensive occurrence at the ice-water interface and diminishing platelet cover towards depth (Figure S6). This has been observed similarly in the Antarctic [*Dayton et al.*, 1969; *Hoppmann et al.*, 2020; *Mahoney et al.*, 2011]. Platelet crystals were largest (up to 15 cm) and most prominent on blocks, ridges, and edges protruding from the level ice, but at close inspection, we found also smaller scale platelet ice crystals (1-2 cm) throughout the bottom of level ice. Also these smaller platelets appeared different from ice lamellae expected in the skeletal layer. We identified no significant spatial difference in under-ice roughness (and thus platelet coverage) from acoustic backscatter derived from the multibeam sonar measurements (Figure S7).

While sheltered areas between ridge keels with low currents seemed to provide best conditions for platelet growth, we observed significant platelet growth of similar size also at locations that were completely exposed to the ice-relative currents (Figure S4) and more than 100m away from any significant ice feature. *Lewis and Milne* [1977] attribute the presence of sub-ice platelet layers to cracks or pressure ridges. While this seems to coincide with the locations of our most prominent observations, we also observed platelet ice far away from such features and can thus neither prove nor rule out the ridge associated ice-pump mechanism of platelet formation as predicted by *Lewis and Perkin* [1986].

We found no direct link between platelet ice distribution and brine drainage features. Despite the occasional observation of brinicles – ice stalactites forming from the contact of descending, cold brine with seawater [*Lewis and Milne*, 1977]– we encountered them both with and without intense platelet ice cover (Figure S8).

3.3 Temporal Variability

During MOSAiC, the ROV diving schedule only allowed for a weekly cycle of repeated visits (Figure S9). Therefore, our information on the temporal variability of platelet ice occurrence is limited and less objective. However, we could identify clear differences in the amount of new platelet ice formation between different periods. These periods were characterized either by new crystal growth, the lack of such, or even a perceived reduction in platelet ice cover. They are identified in Figure 3 to investigate a link between oceanographic conditions and platelet ice formation. As the ROV sampling in the described location only started on 31 December 2019, we cannot provide a detailed assessment of the situation before. However, we observed no platelet ice during ROV dives before 6 December 2019 in a different location approximately 1 km away. We observed platelet ice for the last time during an ROV dive on 28 March 2020, after the floe had been affected by deformation and the return of sunlight. This coincides with the time, when water temperatures under the ice climbed above the local freezing point again (Figure 3c).

3.4 Supercooling

We found supercooled water, the basis for platelet ice formation, well below the ice-water interface, which we confirmed using three different independent measurement platforms. Temperature and salinity data from the ROV, a free-falling Microstructure Sonde (MSS), and several autonomous CTDs deployed at 10 m depth in 10-40 km distance from the ROV site all revealed water temperatures around 0.01-0.02 K below the respective seawater freezing point in the uppermost mixed layer (Figure 3a). This degree of supercooling is similar to observations from the Antarctic [*Mahoney et al.*, 2011] and larger than the calibration uncertainty and uncertainties in the calculation of the local freezing point of seawater. Hence, we can confirm the existence of supercooled water several meters thick as prerequisite for platelet ice formation [*Smith et al.*, 2001]. Measurement uncertainties might however obscure the absolute magnitude and depth of ocean surface supercooling.

Within the mixed layer, the local seawater freezing point is pressure and therefore depth dependent, while temperature and salinity values are approximately constant. Thus, freezing-point departure increases towards the surface with a higher level of supercooling in the uppermost mixed layer right under the ice (Figure 3a,b). This can explain the observed decrease in platelet ice abundance below 2 m depth.

A simple hypothesis for platelet ice growth might thus be that water molecules attach to existing crystallization nuclei e.g. at the ice underside as soon as they are in a strong enough state of supercooling. Considering the turbulent nature of the mixed layer, where water particles get mixed up and down through the entire mixed layer at a time scale of 30 minutes [*Denman and Gargett*, 1983], they oscillate between supercooled and non-supercooled states. Thus, we hypothesize that platelet ice formation is only possible as soon as the temperature in the complete mixed layer lies below the vertically averaged seawater freezing point. This can be either achieved by excessive atmospheric cooling during the Arctic winter [*Danielson et al.*, 2006; *Skogseth et al.*, 2017] or due to a sudden shoaling of the mixed layer, cutting off mixing beyond a certain depth, so that suddenly most of the surface mixed layer has a temperature below the freezing point causing respective formation of platelet ice. Platelet ice could also originate from frazil crystals generated in the water column [*Robinson et al.*, 2020; *Skogseth et al.*, 2017] that rise up and attach to the surface. If present, free floating frazil ice crystals should have been easily detected in light beams used for ROV surveys or Secchi-disk casts. No such enhanced light-scattering by ice crystals was observed but we might have missed it particularly due to temporal limitations of the sampling schedule. Another plausible explanation for platelet formation, lies in the “ice-pump” mechanism [*Lewis and Perkin*, 1983; 1986]: Descending salty brines generated by strong atmospheric cooling in leads or even under a completely closed ice cover can melt deep lying ridge keels and thus supercool the water column and respectively generate platelet ice. Determining the exact nature of the processes involved in the temporally varying strength of platelet ice formation would require more targeted high temporal resolution investigations of platelet growth than could be accomplished during the rigid observational plan for MOSAiC.

Time series of MSS and autonomous observations show that the detected levels of platelet ice were only apparent after a more temporally stable mixed layer with a depth of ~30 m had established in mid-December. Furthermore, the perceived decrease in platelet ice coverage observed in mid-February was likely linked to a passing eddy, decreasing the freezing-point departure in the upper mixed layer (Figure 3b).

Observations of autonomous CTD sensors deployed in the distributed network at 10 to 40 km distance from the central MOSAiC floe (Figure S3) consistently show similar amounts of ocean surface supercooling (Figure 3c). This allows the conclusion that platelet ice formation under Arctic winter sea ice is not a local curiosity, but a widespread, overlooked feature in the Central Arctic Ocean.

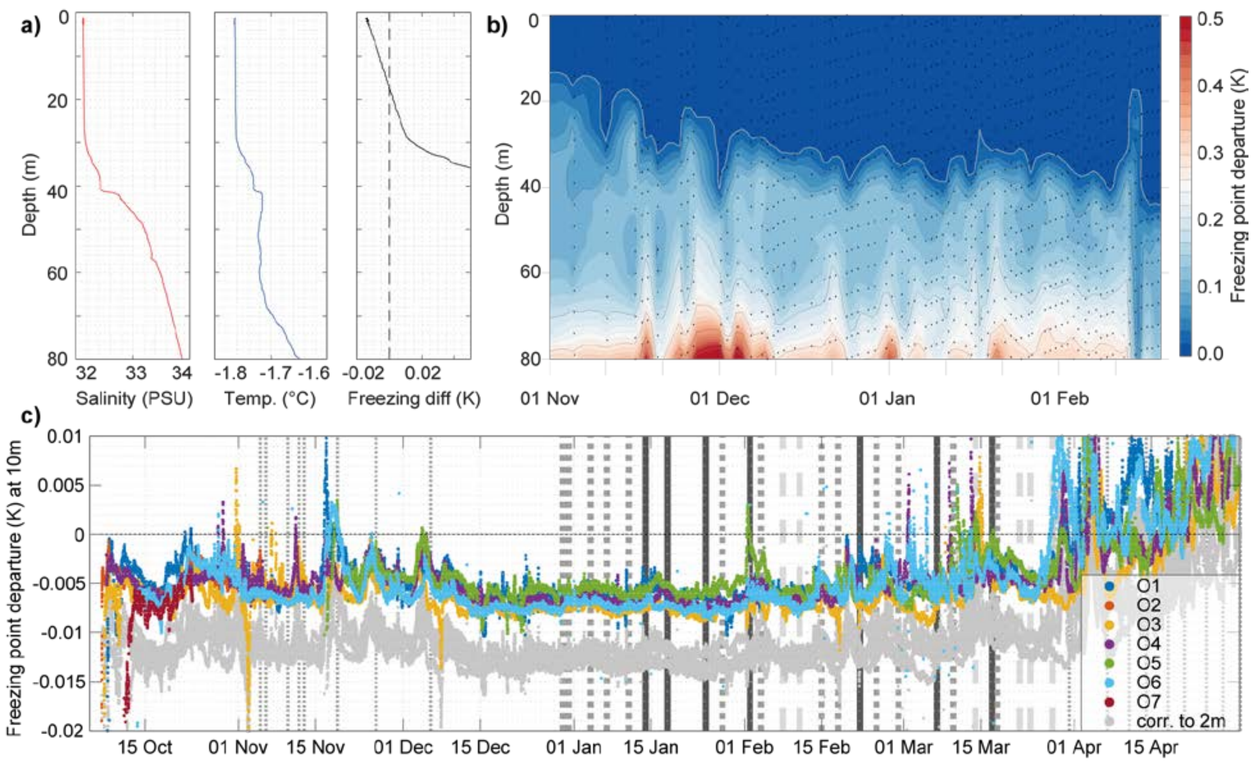

Figure 3. a) Salinity, temperature, and freezing point departure observed by the ROV on 22 February 2020. b) MSS time series of water temperature above the surface freezing point. Note the consistent deepening of the supercooled layer indicated in blue color. c) Time series of freezing-point departure measured in 10 m depth (and adjusted to 2 m depth in gray) from the autonomous observation stations. Vertical lines indicate platelet ice intensity observations classified as high (solid lines), normal (thick dotted lines) and low intensity (dashed lines) based on visual ROV observations. Thin dotted lines indicate ROV surveys without platelet ice observation. See supplemental figure S3 for geometric location of stations relative to the central observatory.

3.5 Persistence in Ice Core Analysis

Despite the ubiquitous occurrence of platelet ice shown in our study, there is a general lack of extensive signs of platelet ice formation in the texture of Arctic sea ice cores of the Transpolar Drift [*Tucker et al.*, 1999]. To further investigate, we retrieved ice cores at three locations (Figure 1b) where we had documented platelet ice beforehand with the ROV cameras. In contrast to most Antarctic landfast ice cores, all of the investigated ice core bottom thin sections (Figure S10) showed only weak signs of incorporated platelet ice. Rapid congelation ice growth of 5-9 cm per week might have concealed a more obvious signature of platelets [*Dempsey et al.*, 2010; *Gough et al.*, 2012]. However, in various places we found a few large, inclined crystals interpreted as originating from platelet crystals. Moreover, during the first leg of MOSAiC at the end of November 2019, an ice core retrieved at the second-year ice site contained more clearly identifiable sections of platelet ice (Figure S11). Thin section analysis indicates substantial microstructural and textural similarities with literature reports of Antarctic platelet ice [*Jeffries et al.*, 1995; *Langhorne et al.*, 2015; *Leonard et al.*, 2006; *Smith et al.*, 2001].

To investigate this more closely, we analyzed the texture of collected platelet crystals refrozen into seawater. The resulting texture (Figure S12) looks significantly different from the one described for freshwater-derived platelet ice by *Jeffries et al.* [1995]. In particular, platelet ice crystals seen from the side have a rectangular rather than triangular shape, and also many platelet crystals exhibit sub-grain boundaries which are described as absent in the work of *Jeffries et al.* [1995].

We thus have two hypotheses why these ubiquitous platelet ice crystals under Arctic winter sea ice do not leave a strong record in the texture of ice cores. First, despite their spectacular voluminous appearance, the ice platelets actually only take up a small volume fraction, so that it is unlikely to observe multiple platelet crystals in a sub-millimeter thick ice core thin section. This has been found also for Antarctic platelet ice incorporated into fast growing congelation ice [*Dempsey et al.*, 2010; *Gough et al.*, 2012]. Second, the platelet crystals may serve as primary nucleation surfaces also for the congelation growth in a way that obscures their initial origin. Both hypotheses could explain why such a widespread cover of sub-ice platelet layers in the winter Arctic has been overlooked in the last decades of sea ice texture investigations.

3.6 Physical, Ecological and Biogeochemical Implications

Considering large scale energy fluxes and the thermodynamics of sea ice growth, platelet ice formation under Arctic sea ice in winter does likely not affect the thermodynamics of sea ice growth significantly. This is particularly due to Arctic platelet ice being a local seasonal phenomenon maintaining a closed energy budget. In contrast, Antarctic platelet ice is often derived from water masses with spatially different origin and thus disrupting the local energy budget. Even though the impact may be small for ice-ocean physics, the porous, ragged structure of the platelet ice interface does affect small scale roughness of the ice underside and will in particular affect the entrainment of water constituents, such as sediments, nutrients, or biological assemblages. One sample of sub-ice platelets from the ROVnet showed elevated levels of halocarbons compared to the general ice column, meaning this sub-ice platelet layer could play a role also in different biogeochemical cycles. Despite the assumed inactivity of the under-ice ecosystem during polar night, platelet ice might still serve as a substrate for algal growth and protection for under-ice macrofauna, as we observed amphipods maneuvering through the maze of crystal blades (Figure S13).

Platelet ice could also play a significant role in the poorly understood consolidation of voids e.g. in sea ice ridges, where it would be able to close large gaps faster than by pure congelation ice growth. This could explain why voids in ridge keels often appeared slushy when drilled through during MOSAiC (Figure S14).

While platelet ice observations in the Arctic date back to the 1970s [*Lewis and Milne*, 1977], the thinner [*Haas et al.*, 2008; *Kwok and Rothrock*, 2009] and more dynamic sea ice [*Kwok et al.*, 2013] of recent years might increase rapid cooling of Arctic surface waters and thus promote platelet ice formation.

4. Summary

During the polar night of the international drift expedition MOSAiC in 2019-2020, we observed a widespread coverage of the ice underside with a sub-ice platelet layer. These up to 15 cm large platelet ice crystals grew in situ from supercooled water of the uppermost mixed-layer, both on exposed ice features and level ice. This is the first comprehensive in situ observation of sub-ice platelet layer formation during Arctic winter in the free-drifting ice of the Central Arctic. As historic observations show, this is not a new phenomenon but only modern robotic equipment at a winter drift ice station allowed for its detailed observation.

Platelet ice formation has been overlooked so far as a widespread feature of ice growth during Arctic winter. Our study provides the first observational evidence for a link between platelet growth intensity, mixed layer stability and supercooling, but the detailed processes with respect to their seasonal impacts on ice-ocean interactions are yet to be understood. In particular, we were able to show that this sub-ice platelet layer does not always leave a clear imprint on sea-ice texture and was hence easily overlooked in past ice core analyses (Figure S15).

The potential importance of sub-ice platelet layers for the ice-associated ecosystem and biogeochemical fluxes during Arctic winter should be investigated more closely in the future. To improve our understanding of the involved physical processes, we suggest a more targeted investigation during future Arctic winter campaigns with the goal to achieve higher temporal resolution and more objective observations of platelet crystal growth. This could be achieved by fixed underwater cameras in relation to water dynamics, potential ridge keel melting and thermodynamics in the mixed layer.

Data availability statement

Data used in this manuscript were produced as part of the international Multidisciplinary drifting Observatory for the Study of the Arctic Climate (MOSAiC) with the tag MOSAiC20192020. All data is archived in the MOSAiC Central Storage (MCS) and will be available on PANGAEA after finalization of the respective datasets according to the MOSAiC data policy. Screenshots from ROV video [*Katlein et al.*, 2020d], acoustic backscatter [*Katlein et al.*, 2020b], ice core data [*Katlein et al.*, 2020c] and ROV CTD data [*Katlein et al.*, 2020a] are already available on PANGAEA. Oceanographic data from autonomous platforms 2019O1-201908 can be accessed at seaiceportal.de. Ice and snow thickness data were kindly provided by Stefan Hendricks.

Acknowledgments

We are thankful to all members of the MOSAiC collaboration who made this unique expedition possible. We want to thank all people enabling the MOSAiC ROV and buoy programs at AWI, in particular Julia Regnery, Kathrin Riemann-Campe, Martin Schiller, Anja Nicolaus, Dirk Kalmbach. Furthermore, we thank Johannes Lemburg from the AWI workshop and Hauke Flores for providing the ROVnet. We also thank the Captain, Crew and Chief Scientists of RV Polarstern and support icebreakers IB Kapitan Dranitsyn and RV Akademik Fedorov for their support (Project ID: AWI_PS122_00). The participation of Dmitry V. Divine in the MOSAiC expedition was supported by Research Council of Norway project HAVOC (No. 280292) and project DEARice supported by EU ARICE program (EU grant agreement No. 730965). Participation of Ilkka Matero was supported by the Diatom ARCTIC project (BMBF grant, 03F0810A), part of the Changing Arctic Ocean programme, jointly funded by the UKRI Natural Environment Research Council (NERC) and the German Federal Ministry of Education and Research (BMBF). Stefanie Arndt was funded by the German Research Council (DFG) in the framework of the priority program ‘‘Antarctic Research with comparative investigations in Arctic ice areas’’ by grant to SPP1158. We thank one anonymous reviewer and Pat Langhorne for improving this manuscript during the peer-review process.

This study was funded by the Alfred-Wegener-Institut Helmholtz-Zentrum für Polar- und Meeresforschung and the Helmholtz Research program PACES II. Operation and development of the ROV were supported by the Helmholtz Infrastructure Initiative “Frontiers in Arctic Marine Monitoring (FRAM)”.

References

Arrigo, K. R., T. Mock, and M. P. Lizotte (2010), Primary Producers and Sea Ice, in *Sea Ice*, edited by D. G. S. Thomas N.D. , pp. 283-325, doi:10.1002/9781444317145.ch8.

Bardout, G., E. Périé, and B. Poyelle (2011), *On a marché sous le pôle : Deepsea under the Pole*, Chêne, [Paris].

Carnat, G., T. Papakyriakou, N. X. Geilfus, F. Brabant, B. Delille, M. Vancoppenolle, G. Gilson, J. Zhou, and J.-L. Tison (2017), Investigations on physical and textural properties of Arctic first-year sea ice in the Amundsen Gulf, Canada, November 2007–June 2008 (IPY-CFL system study), *J. Glaciol.*, *59*(217), 819-837, doi:10.3189/2013JoG12J148.

Danielson, S., K. Aagaard, T. Weingartner, S. Martin, P. Winsor, G. Gawarkiewicz, and D. Quadfasel (2006), The St. Lawrence polynya and the Bering shelf circulation: New observations and a model comparison, *Journal of Geophysical Research: Oceans*, *111*(C9), doi:10.1029/2005jc003268.

Dayton, P. K., G. A. Robilliard, and A. L. Devries (1969), Anchor Ice Formation in McMurdo Sound, Antarctica, and Its Biological Effects, *Science*, *163*(3864), 273-274, doi:10.1126/science.163.3864.273.

Dempsey, D. E., P. J. Langhorne, N. J. Robinson, M. J. M. Williams, T. G. Haskell, and R. D. Frew (2010), Observation and modeling of platelet ice fabric in McMurdo Sound, Antarctica, *Journal of Geophysical Research: Oceans*, *115*(C1), doi:10.1029/2008jc005264.

Denman, K. L., and A. E. Gargett (1983), Time and space scales of vertical mixing and advection of phytoplankton in the upper ocean, *Limnol. Oceanogr.*, *28*(5), 801-815, doi:10.4319/lo.1983.28.5.0801.

Dieckmann, G., G. Rohardt, H. Hellmer, and J. Kipfstuhl (1986), The occurrence of ice platelets at 250 m depth near the Filchner Ice Shelf and its significance for sea ice biology, *Deep Sea Research Part A. Oceanographic Research Papers*, *33*(2), 141-148, doi:https://doi.org/10.1016/0198-0149(86)90114-7.

Dowdeswell, J. A., and M. O. Jeffries (2017), Arctic Ice Shelves: An Introduction, in *Arctic Ice Shelves and Ice Islands*, edited by L. Copland and D. Mueller, pp. 3-21, Springer Netherlands, Dordrecht, doi:10.1007/978-94-024-1101-0_1.

Eicken, H. (1994), Structure of under-ice melt ponds in the central Arctic and their effect on, the sea-ice cover, *Limnol. Oceanogr.*, *39*(3), 682-693, doi:10.4319/lo.1994.39.3.0682.

Eicken, H., and M. Salganek (2010), *Field Techniques for Sea-Ice Research*, University of Alaska Press.

Gough, A. J., A. R. Mahoney, P. J. Langhorne, M. J. M. Williams, N. J. Robinson, and T. G. Haskell (2012), Signatures of supercooling: McMurdo Sound platelet ice, *J. Glaciol.*, *58*(207), 38-50, doi:10.3189/2012JoG10J218.

Günther, S., and G. S. Dieckmann (2004), Seasonal development of algal biomass in snow-covered fast ice and the underlying platelet layer in the Weddell Sea, Antarctica, *Antarctic Science*, *11*(3), 305-315, doi:10.1017/S0954102099000395.

Haas, C., A. Pfaffling, S. Hendricks, L. Rabenstein, J.-L. Etienne, and I. Rigor (2008), Reduced ice thickness in Arctic Transpolar Drift favors rapid ice retreat, *Geophys. Res. Lett.*, *35*(17), L17501, doi:10.1029/2008gl034457.

Hoppmann, M., et al. (2017), Ice platelets below Weddell Sea landfast sea ice, *Ann. Glaciol.*, *56*(69), 175-190, doi:10.3189/2015AoG69A678.

Hoppmann, M., M. E. Richter, I. J. Smith, S. Jendersie, P. J. Langhorne, N. D. Thomas, and G. S. Dieckmann (2020), Platelet ice, the Southern Ocean's hidden ice: a review, *Ann. Glaciol.*

Hunkeler, P. A., M. Hoppmann, S. Hendricks, T. Kalscheuer, and R. Gerdes (2016), A glimpse beneath Antarctic sea ice: Platelet layer volume from multifrequency electromagnetic induction sounding, *Geophys. Res. Lett.*, *43*(1), 222-231, doi:10.1002/2015gl065074.

Jeffries, M. O., K. Schwartz, K. Morris, A. D. Veazey, H. R. Krouse, and S. Gushing (1995), Evidence for platelet ice accretion in Arctic sea ice development, *Journal of Geophysical Research: Oceans*, *100*(C6), 10905-10914, doi:10.1029/95jc00804.

Katlein, C., P. Anhaus, I. Matero, and M. Nicolaus (2020a), Pressure, temperature, conductivity and dissolved oxygen raw data during ROV dives from POLARSTERN cruise PS122/2, links to files, edited, PANGAEA.

Katlein, C., P. M. Anhaus, Ilkka, and M. Nicolaus (2020b), Sea ice draft and acoustic backscatter (240kHz) raw data derived from multibeam sonar during the ROV BEAST dive PS122/2_18-19, edited, PANGAEA, doi:10.1594/PANGAEA.917498.

Katlein, C., P. Itkin, and D. V. Divine (2020c), Salinity measured on sea ice core PS122/2_24-114 during MOSAiC Leg 2, edited, PANGAEA, doi:10.1594/PANGAEA.919474.

Katlein, C., D. Krampe, and M. Nicolaus (2020d), Extracted frames from main ROV camera videos during MOSAiC Leg 2, edited, PANGAEA, doi:10.1594/PANGAEA.919398.

Katlein, C., M. Schiller, H. J. Belter, V. Coppolaro, D. Wenslandt, and M. Nicolaus (2017), A New Remotely Operated Sensor Platform for Interdisciplinary Observations under Sea Ice, *Frontiers in Marine Science*, *4*(281), doi:10.3389/fmars.2017.00281.

Kirillov, S., I. Dmitrenko, S. Rysgaard, D. Babb, J. Ehn, J. Bendtsen, W. Boone, D. Barber, and N. Geilfus (2018), The Inferred Formation of a Subice Platelet Layer Below the Multiyear Landfast Sea Ice in the Wandel Sea (NE Greenland) Induced by Meltwater Drainage, *Journal of Geophysical Research: Oceans*, *123*(5), 3489-3506, doi:10.1029/2017jc013672.

Knust, R. (2017), Polar Research and Supply Vessel POLARSTERN operated by the Alfred-Wegener-Institute, *Journal of large-scale research facilities JLSRF*, *3*, doi:10.17815/jlsrf-3-163.

Krumpen, T., et al. (2020), The MOSAiC ice floe: sediment-laden survivor from the Siberian shelf, *The Cryosphere Discuss.*, *2020*, 1-20, doi:10.5194/tc-2020-64.

Kwok, R., and D. A. Rothrock (2009), Decline in Arctic sea ice thickness from submarine and ICESat records: 1958-2008, *Geophys. Res. Lett.*, *36*, doi:10.1029/2009gl039035.

Kwok, R., G. Spreen, and S. Pang (2013), Arctic sea ice circulation and drift speed: Decadal trends and ocean currents, *Journal of Geophysical Research: Oceans*, *118*(5), 2408-2425, doi:10.1002/jgrc.20191.

Langhorne, P. J., et al. (2015), Observed platelet ice distributions in Antarctic sea ice: An index for ocean-ice shelf heat flux, *Geophys. Res. Lett.*, *42*(13), 5442-5451, doi:10.1002/2015gl064508.

Leonard, G. H., C. R. Purdie, P. J. Langhorne, T. G. Haskell, M. J. M. Williams, and R. D. Frew (2006), Observations of platelet ice growth and oceanographic conditions during the winter of 2003 in McMurdo Sound, Antarctica, *Journal of Geophysical Research: Oceans*, *111*(C4), doi:10.1029/2005jc002952.

Lewis, E. L., and R. A. Lake (1971), Sea ice and supercooled water, *Journal of Geophysical Research (1896-1977)*, *76*(24), 5836-5841, doi:10.1029/JC076i024p05836.

Lewis, E. L., and A. R. Milne (1977), Underwater sea ice formation in “Polar Oceans,” paper presented at Proc. SCOR/SCAR Polar Oceans Conference, Arctic Institute North America.

Lewis, E. L., and R. G. Perkin (1983), Supercooling and energy exchange near the Arctic Ocean surface, *Journal of Geophysical Research: Oceans*, *88*(C12), 7681-7685, doi:10.1029/JC088iC12p07681.

Lewis, E. L., and R. G. Perkin (1986), Ice pumps and their rates, *Journal of Geophysical Research: Oceans*, *91*(C10), 11756-11762, doi:10.1029/JC091iC10p11756.

Lofgren, G., and W. F. Weeks (2017), Effect of Growth Parameters on Substructure Spacing in NaCl Ice Crystals, *J. Glaciol.*, *8*(52), 153-164, doi:10.3189/S0022143000020827.

Mahoney, A. R., A. J. Gough, P. J. Langhorne, N. J. Robinson, C. L. Stevens, M. M. J. Williams, and T. G. Haskell (2011), The seasonal appearance of ice shelf water in coastal Antarctica and its effect on sea ice growth, *Journal of Geophysical Research: Oceans*, *116*(C11), doi:10.1029/2011jc007060.

Martin, S., and P. Kauffman (2006), The evolution of under-ice melt ponds, or double diffusion at the freezing point, *Journal of Fluid Mechanics*, *64*(3), 507-528, doi:10.1017/S0022112074002527.

Notz, D., M. G. McPhee, M. G. Worster, G. A. Maykut, K. H. Schlünzen, and H. Eicken (2003), Impact of underwater-ice evolution on Arctic summer sea ice, *Journal of Geophysical Research: Oceans*, *108*(C7), doi:10.1029/2001jc001173.

Pfirman, S., W. Haxby, H. Eicken, M. Jeffries, and D. Bauch (2004), Drifting Arctic sea ice archives changes in ocean surface conditions, *Geophys. Res. Lett.*, *31*(19), n/a-n/a, doi:10.1029/2004GL020666.

Ragobert, T., et al. (2008), Tara : journey to the heart of the climate machine, edited.

Robinson, N. J., B. S. Grant, C. L. Stevens, C. L. Stewart, and M. J. M. Williams (2020), Oceanographic observations in supercooled water: Protocols for mitigation of measurement errors in profiling and moored sampling, *Cold Reg. Sci. Tech.*, *170*, 102954, doi:https://doi.org/10.1016/j.coldregions.2019.102954.

Rutter, J. W., and B. Chalmers (1953), A PRISMATIC SUBSTRUCTURE FORMED DURING SOLIDIFICATION OF METALS, *Canadian Journal of Physics*, *31*(1), 15-39, doi:10.1139/p53-003.

Shokr, M., and N. Sinha (2015), *Sea Ice: Physics and Remote Sensing*, 1-579 pp., doi:10.1002/9781119028000.

Skogseth, R., F. Nilsen, and L. H. Smedsrud (2017), Supercooled water in an Arctic polynya: observations and modeling, *J. Glaciol.*, *55*(189), 43-52, doi:10.3189/002214309788608840.

Smith, I., P. Langhorne, T. Haskell, H. Trodahl, R. Frew, and R. Vennell (2001), Platelet ice and the land-fast sea ice of McMurdo Sound, Antartica, *Ann. Glaciol.*, *33*, 21-27, doi:10.3189/172756401781818365.

Thomas, D. N., and G. S. Dieckmann (2002), Biogeochemistry of Antarctic sea ice, *Oceanography and marine biology*, *40*, 143-170.

Tucker, W. B., A. J. Gow, D. A. Meese, H. W. Bosworth, and E. Reimnitz (1999), Physical characteristics of summer sea ice across the Arctic Ocean, *Journal of Geophysical Research: Oceans*, *104*(C1), 1489-1504, doi:10.1029/98jc02607.

Vacchi, M., A. L. DeVries, C. W. Evans, M. Bottaro, L. Ghigliotti, L. Cutroneo, and E. Pisano (2012), A nursery area for the Antarctic silverfish Pleuragramma antarcticum at Terra Nova Bay (Ross Sea): first estimate of distribution and abundance of eggs and larvae under the seasonal sea-ice, *Polar Biol.*, *35*(10), 1573-1585, doi:10.1007/s00300-012-1199-y.

Weeks, W. F., and S. F. Ackley (1986), The Growth, Structure, and Properties of Sea Ice, in *The Geophysics of Sea Ice*, edited by N. Untersteiner, pp. 9-164, Springer US, Boston, MA, doi:10.1007/978-1-4899-5352-0_2.

WMO (2014), *JCOMM Expert Team on Sea Ice: Sea-Ice Nomenclature: snapshot of the WMO Sea Ice Nomenclature WMO No. 259, volume 1 – Terminology and Codes; Volume II – Illustrated Glossary and III – International System of Sea-Ice Symbols*, WMO-JCOMM, Geneva, Switzerland, doi:http://hdl.handle.net/11329/328.

Wollenburg, J. E., M. Iversen, C. Katlein, T. Krumpen, M. Nicolaus, G. Castellani, I. Peeken, and H. Flores (2020), New observations of the distribution, morphology and dissolution dynamics of cryogenic gypsum in the Arctic Ocean, *The Cryosphere*, *14*(6), 1795-1808, doi:10.5194/tc-14-1795-2020.

Zubov, N. N. (1963), Arctic ice.

Geophysical Research Letters

Supporting Information for

Platelet Ice under Arctic Pack Ice in Winter

Christian Katlein[1*], Volker Mohrholz[2], Igor Sheikin[3], Polona Itkin[4], Dmitry V. Divine[5], Julienne Stroeve[6,7], Arttu Jutila[1], Daniela Krampe[1], Egor Shimanchuk[3], Ian Raphael[8], Benjamin Rabe[1], Ivan Kuznetsov[1], Maria Mallet[1], Hailong Liu[9], Mario Hoppmann[1], Ying-Chih Fang[1], Adela Dumitrascu[10], Stefanie Arndt[1], Philipp Anhaus[1], Marcel Nicolaus[1], Ilkka Matero[1], Marc Oggier[11], Hajo Eicken[11], Christian Haas[1]

[1]Alfred-Wegener-Institute Helmholtz Center for Polar and Marine Research, Bremerhaven, Germany

[2]Institut für Ostseeforschung, Warnemünde, Germany.

[3]Arctic and Antarctic Research Institute, St.Petersburg, Russia

[4]UiT University of Tromsø, Tromsø, Norway

[5]Norwegian Polar Institute, Tromsø, Norway

[6]University College of London, London, United Kingdom

[7]Center for Earth Observation Science, Department of Environment & Geography, University of Manitoba, Winnipeg, MB, Canada

[8]Thayer School of Engineering, Dartmouth College, Hanover NH, United States of America

[9]Shanghai Jiao Tong University, Shanghai, China

[10]University of Gothenburg, Gothenburg, Sweden

[11]International Arctic Research Center, University of Alaska Fairbanks, Fairbanks AK, United States of America

Contents of this file

Introduction

This supplementary information provides additional text and graphics – mostly images – to further illustrate the platelet ice observations described in the main paper. All raw data used in this study are archived in the MOSAiC Central Storage (MCS) according to the MOSAiC Data Policy at the Alfred-Wegener-Institute (AWI) and will be accessible unrestricted after the 1 January 2023.

Text S1: Precision of CTD instruments

The observed supercooling of 10 to 20 mK is close to the uncertainty of the used instruments. Typical uncertainties for temperature, pressure, and salinity derived from conductivity sensors are 5 mK, 0.2 dbar and 0.01 g/kg, respectively. All instruments were calibrated prior to the expedition in calibration labs of the particular manufacturer. The pressure sensor of the MSS was checked by comparing data collected in air above the surface. The observed offset was applied during post processing. The temperature sensors of the MSS were checked against a Seabird SBE911+ CTD system. For this purpose the MSS was mounted on the CTD/rosette frame to gather a concurrent profile of both instruments in the upper 200 m. The SBE911+ will only be finally calibrated several months after the MOSAiC expedition using an analysis of water samples from the rosette with a high-precision salinometer, and calibration of the temperature and conductivity sensors by the manufacturer. Hence, we will only be able to carry out our cross-calibration after that time.
The MSS consists of two temperature sensors, a high precise PT100 and a fast FP07. The sensors were calibrated by Sea & Sun Technology GmbH on 25 May 2019. The calibration range of both temperature sensors is 0 to 30°C. Although, the surface temperature was about -1.7°C and beyond the calibration range, the very linear characteristic of the platinum wire PT100 sensor allow reliable measurements in this range. The uncertainties of the PT100 and the FP07 after the calibration were given by the manufacturer with 2 mK. The uncertainties of pressure and conductivity sensor were given with 0.05 dbar and 0.001 mS/cm, respectively.

The in-situ freezing temperature was calculated with TEOS-10 toolbox GWS [*McDougall and Barker*, 2011]. It depends on absolute salinity and pressure. A salinity uncertainty of 0.01 g/kg results in an uncertainty of freezing temperature of 0.5 mK. The pressure uncertainty of 0.2 dbar causes a freezing temperature uncertainty of 0.15 mK. Thus, the uncertainty of the calculated freezing temperature is not critical, and lower than 1mK.
By using two independent temperature sensors, with different physical measuring principles (platinum wire, and NTC semiconductor element) a failure or drift of one sensor is easily observed. It is very unlikely that both sensors depict the same bias or drift concurrently. To check the sensors the FP07 readings were low pass filtered with the time constant of the PT100. Then the difference between both sensors was calculated. During our campaign no significant change of the temperature difference between both sensors was observed. Thus, we assume an uncertainty of the MSS temperature readings below 5 mK.

Icing of the sensors in supercooled water was not observed, and is highly unlikely. The MSS was operated from a heated tent with about 5°C. Each MSS deployment consists of four to ten subsequent profiles down to 400 m depth. Since only the upper 15 to 25 m are below the in-situ freezing temperature the probe is most of the time (>93%) in warmer water layers. The time in the supercooled surface layer was 80 to 90 s for each profile.

Several salinity and temperature measurements used in this study are from autonomous ice-tethered instrument systems (hereafter named "buoys"). These buoys contain a surface unit for data telemetry (IRIDIUM) and position (GPS), a 100 m long conducting tether, a terminal weight and five inductive Seabird Microcat CTD (SBE 37IM) between the end of the tether and 10 m water depth. The full buoys (model PacificGyre SVP5S) were custom-designed in cooperation with the Alfred-Wegener-Institute and manufactured by Pacific Gyre Inc. (Oceanside, USA). The Microcat CTD were calibrated by Seabird prior to assembly into the buoy. For the SBE 37IM the manufacturer states an accuracy for the temperature sensor of ± 2mK and a resolution of 0. 1 mK with a stability of 0. 2 mK per month. This results in a maximum expected error of about 5 mK, similar to that of the MSS. The salinity and pressure errors result in an error in the freezing temperature that is similarly negligible as for the MSS. The uppermost CTD in all buoys reported such a low temperature, giving further confidence in our observations of supercooling.
Several profiles with a small, mobile CTD system were obtained nearby some of those buoys throughout the year. This will be used for cross-calibration several months after the MOSAiC expedition, once all main CTD systems used during MOSAiC have been finally calibrated. Even without final calibration, we can say with similar confidence as for the MSS data that we measured supercooled water, as presented in this work.

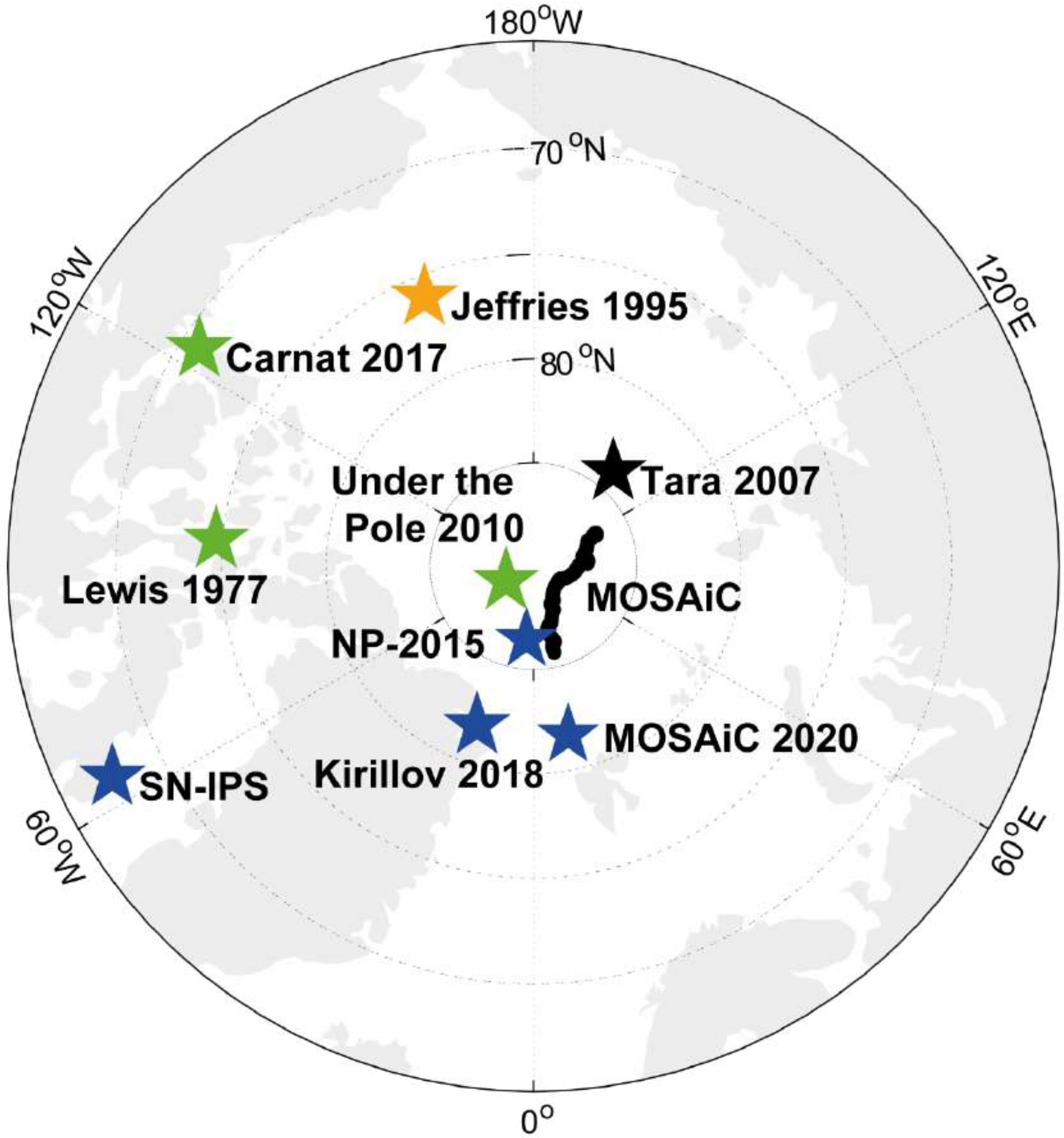

Figure S1. Map showing previous observations of platelet ice with their geographic reference and season (stars indicate location and black, green, blue, orange colors the winter, spring, summer, fall season, respectively). Seasons are indicated as platelet ice formation in summer will in most cases result from meltwater percolation, and thus an entirely different process. The black line shows the track during which platelet ice was observed in this study. Observation references and details can be found in Table ST1.

Table ST1. Collection of previous descriptions of platelet ice in the Arctic. The table includes all observations known to the authors, excluding observations that are explicitly described as false bottom formations in under-ice melt-ponds. It should be noted that most summer season observations likely differ significantly in formation mechanism from our winter observations presented in this study. This also applies to the observation of melt-induced sub-ice platelet layer formation observed on the MOSAiC floe in the end of June 2020.

Work	Reference	Region	Season	Comment
Lewis et al.	*[Lewis and Milne, 1977]*	Resolute Bay (?)	April (?)	time and region not explicitly specified
Jeffries et al.	*[Jeffries et al., 1995]*	Beaufort Sea	August/ September	second and multi-year ice cores
Tara drift	*[Ragobert et al., 2008]*	Central Arctic	Winter	diving observations
“Under the Pole” expedition	*[Bardout et al., 2011]*	Central Arctic	April	exact location unclear
North Pole-2015	*I. Sheikin personal observation*	Central Arctic	July	underwater camera observation
Carnat et al.	*[Carnat et al., 2017]*	Amundsen Gulf	mid-March & mid-May	ice cores - before melt-onset
Kirilov et al.	*[Kirillov et al., 2018]*	Wandel Sea	July/August	indirect buoy observation
Sentinel North – IPS 2018 (CCGS Amundsen)	*C. Katlein personal observation*	southern Baffin Bay	July	edges of melted-through melt ponds
MOSAiC Leg 4	*G. Castellani personal communication*	Northern Fram Strait	end-June	formed after significant surface melt.
MOSAiC Leg 2&3	*this study*	Central Arctic	December to March	

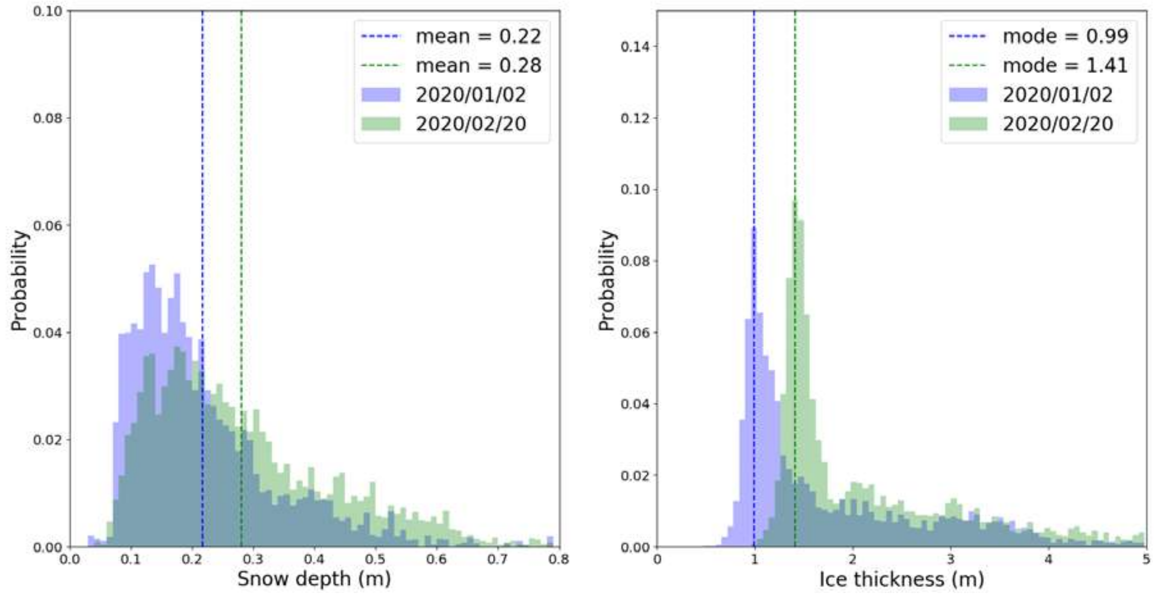

Figure S2. Snow (left) and ice thickness (right) distributions as measured by a Magna Probe (Snow Hydro) and an electromagnetic sounding device GEM-2 (Geophex) on the two main transect loops on the MOSAiC floe. Blue colors indicate a survey from 2 January 2020 coinciding with the first platelet ice observations, while green colors represent the situation on 20 February 2020. Data provided by Stefan Hendricks, AWI.

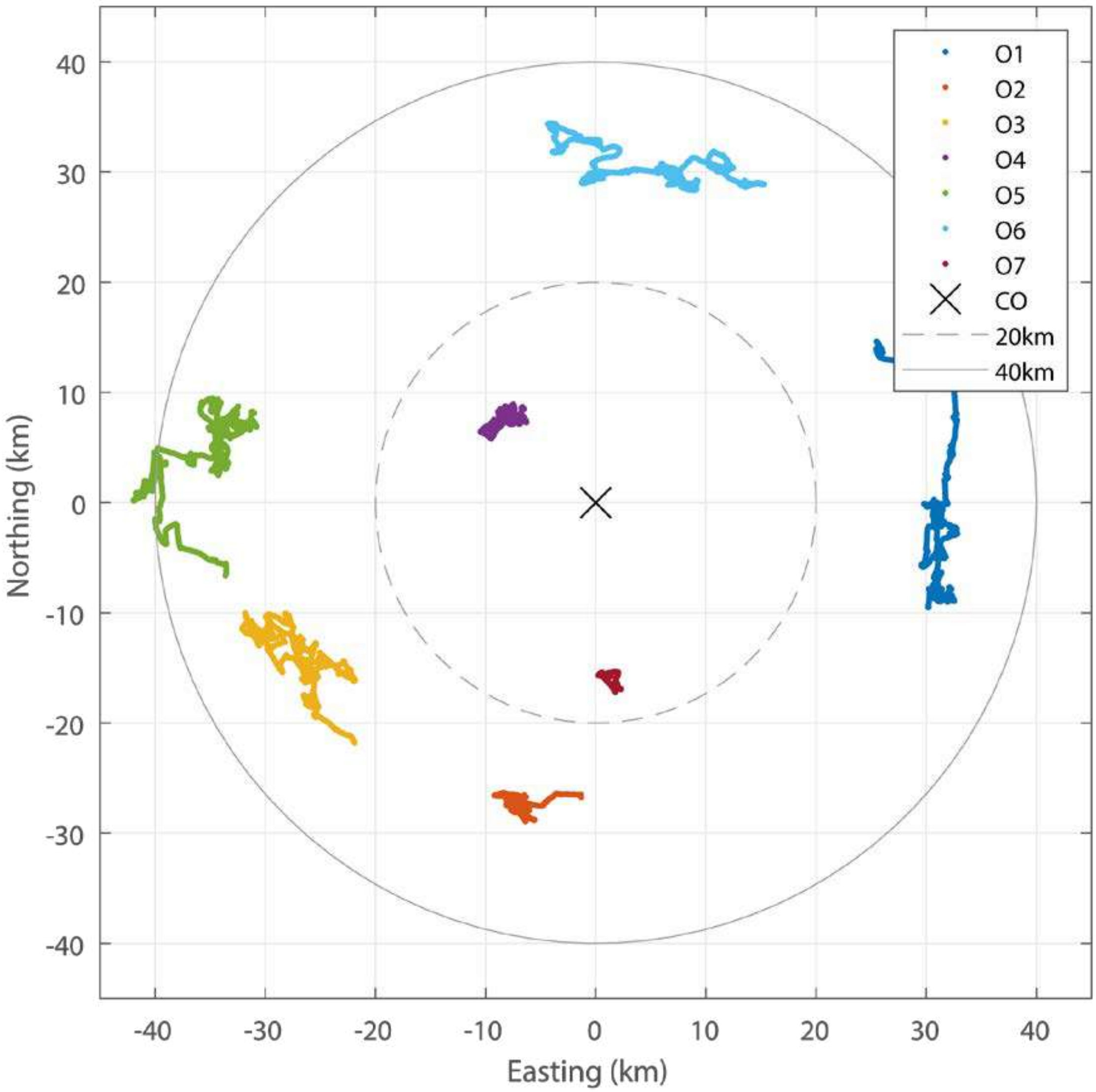

Figure S3. Relative locations of oceanographic autonomous observatories (O1-O7) in relation to the MOSAiC central observatory (CO). Plot is corrected for apparent rotation, as the MOSAiC floe drifts across a wide range of latitudes.

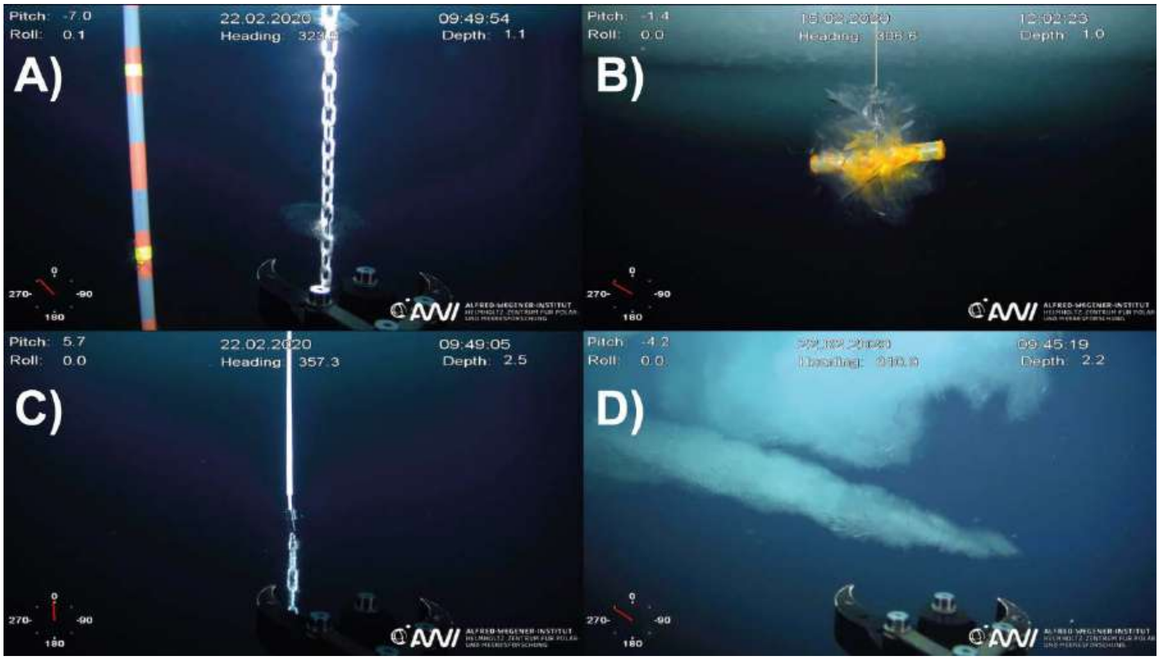

Figure S4. A) A 12 cm large single platelet crystal intergrown into a stainless steel chain. B) Platelet crystals growing around the 20 cm long steel cross-bar of a hot-wire. C) Thermistor chain covered in polymer heat-shrink. Note the absence of platelet ice on the plastic surface. D). Platelet crystals growing on an extended spike without any shelter from strong currents.

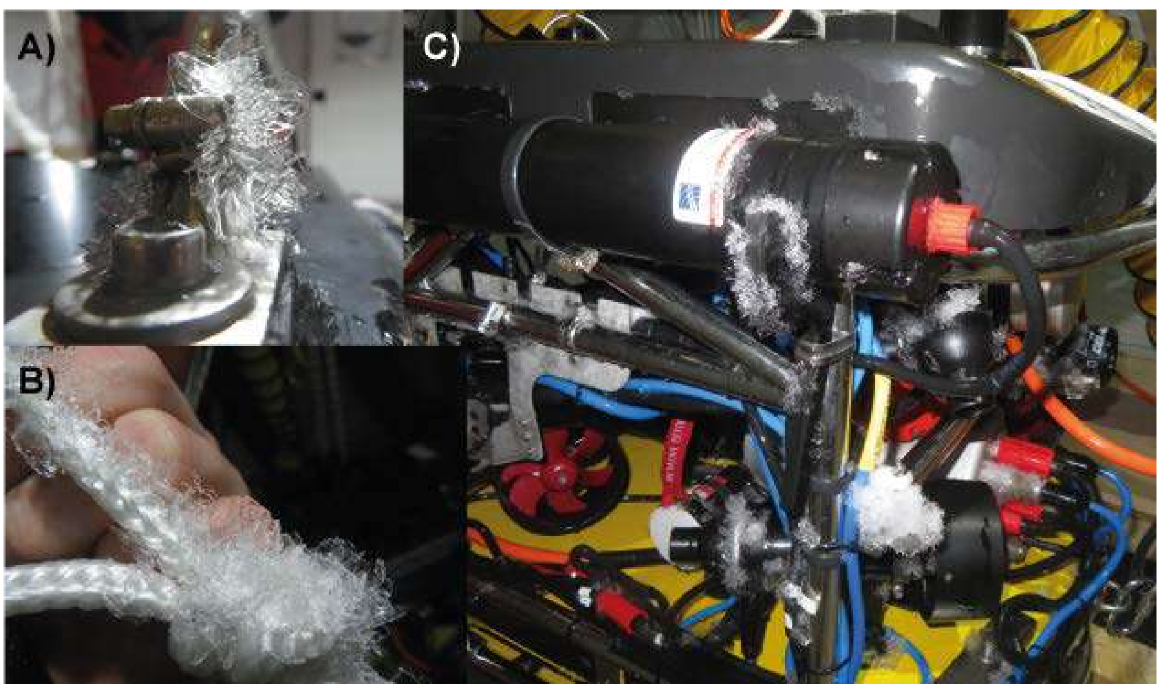

Figure S5. Platelet ice crystal growth on the ROV system: A) Close-up of small crystals on the ROV, B) Crystals growing on the attachment rope. C) Platelet growth on the edges and corners of the ROV system.

Figure S6. Vertical gradient of platelet ice growth on a chain.

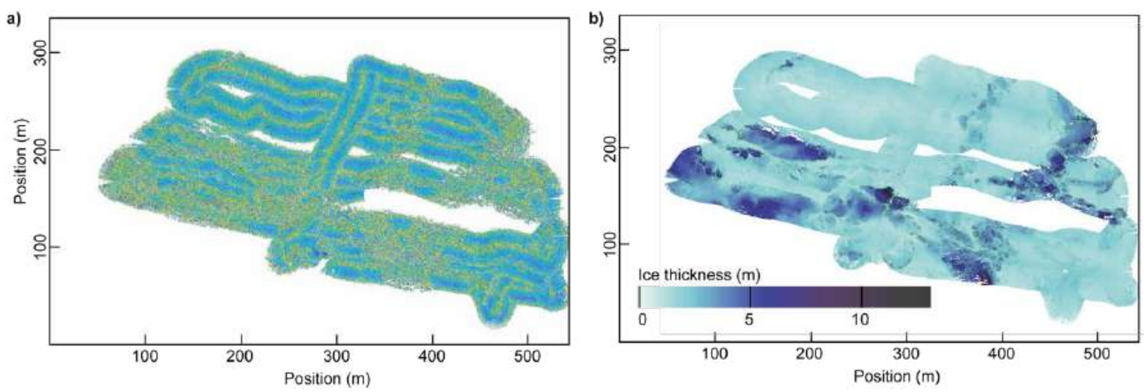

Figure S7. a) Map of raw acoustic backscatter intensity measurements on 31 December 2019. Data are not corrected for across-track incidence angle differences. Bright colors correspond to high backscatter. Regions of generally elevated backscatter are co-located with ridges as shown in the corresponding ice draft map in b). Data are available at https://doi.pangaea.de/10.1594/PANGAEA.917498.

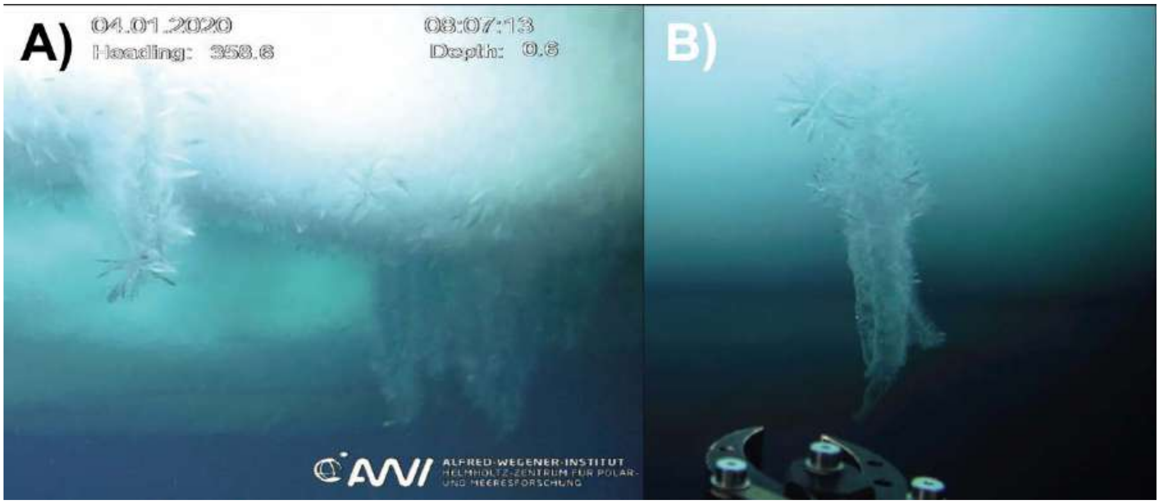

Figure S8. Brinicles under the ice observed surrounded with (A) and without (B) extensive platelet ice coverage.

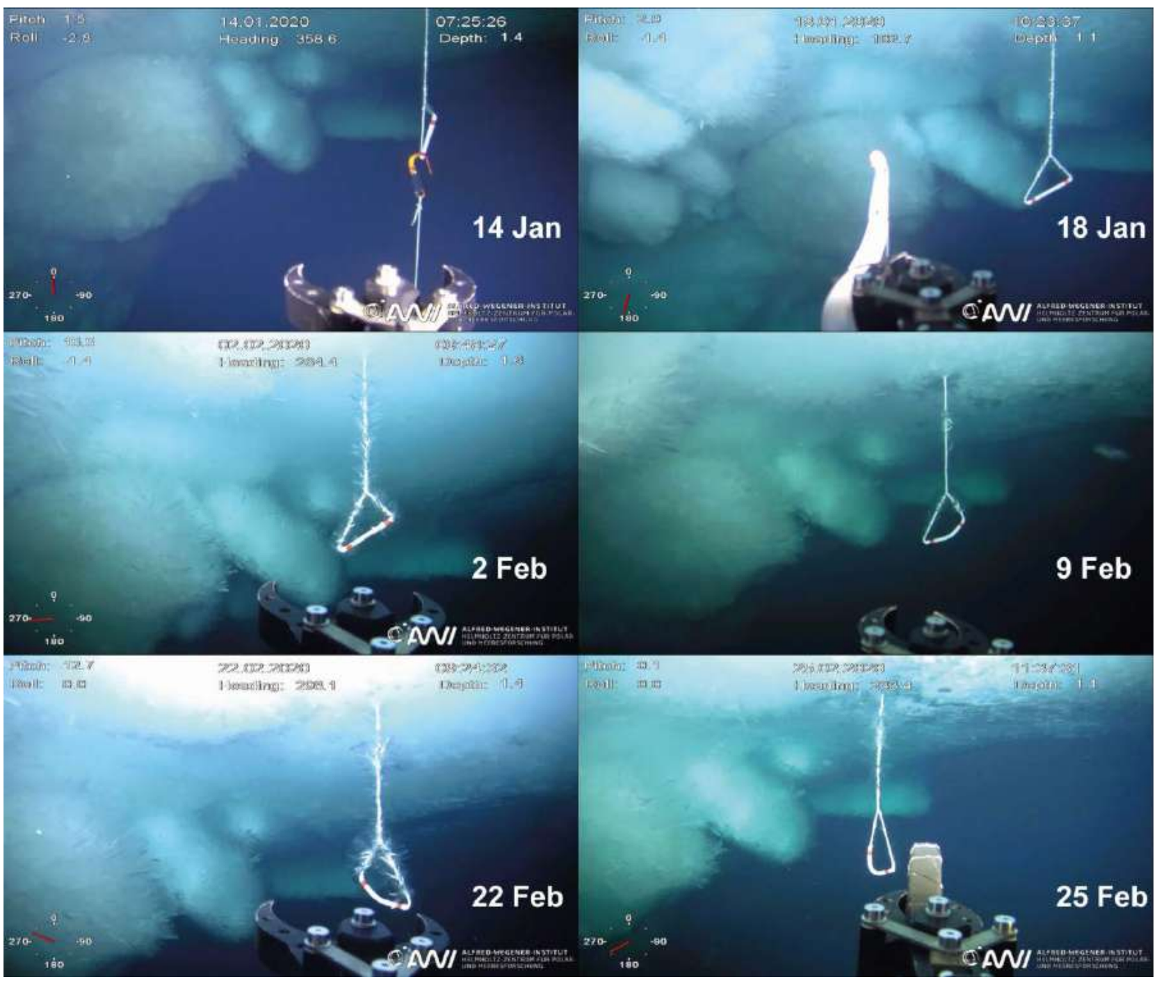

Figure S9. Time series of under-ice photographs showing the development of platelet ice on ridge blocks and a rope sling deployed next to the ridge observatory. All pictures are available at https://doi.pangaea.de/10.1594/PANGAEA.919398.

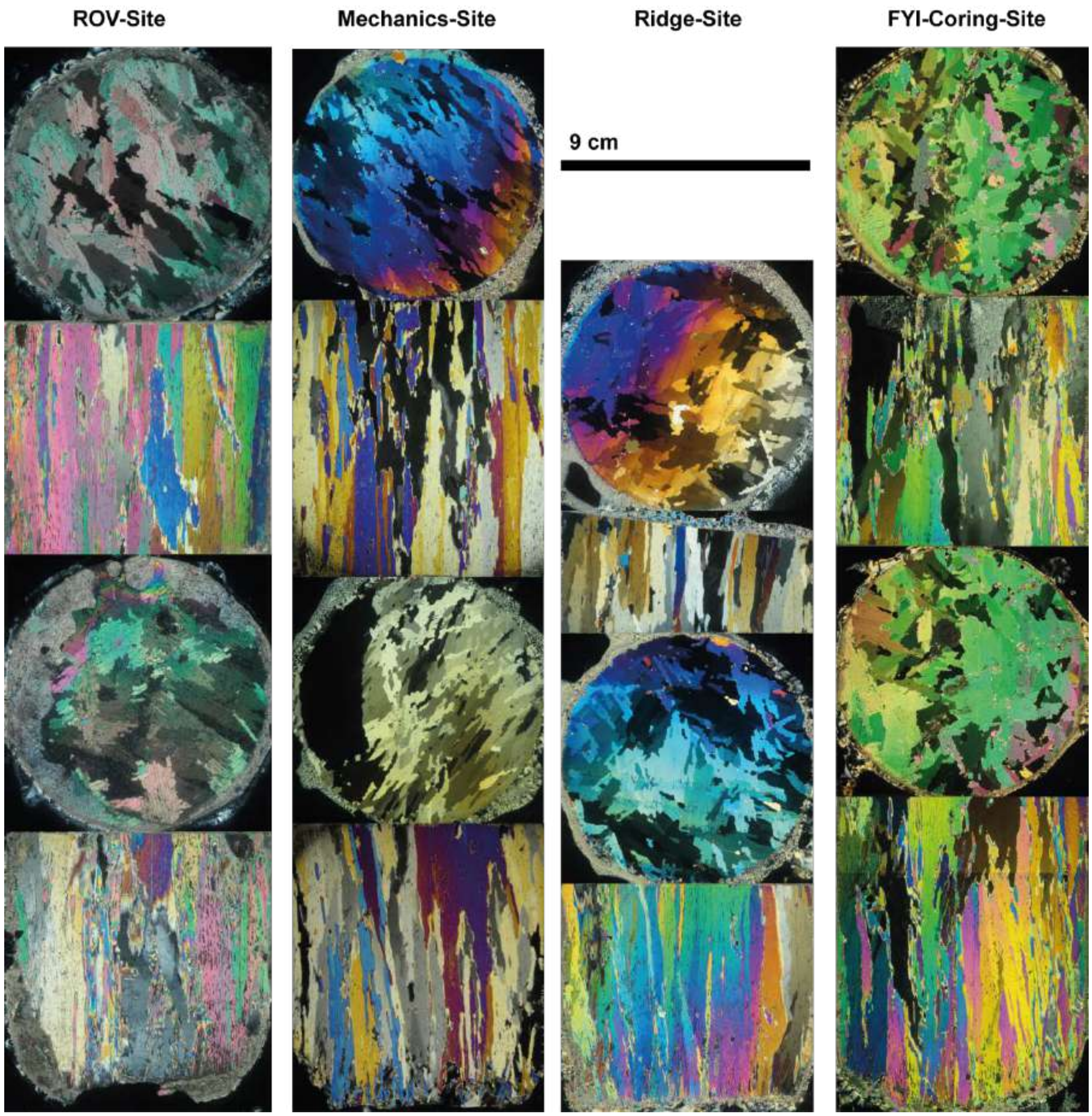

Figure S10. Thin sections of ice cores taken in the end of February photographed between crossed polarizers: horizontal (circular) and vertical thin sections of the two bottommost segments of retrieved ice cores on second year ice (thickness 1.8 m) near the ROV deployment site (left), second year ice (thickness 1.27 m) at the mechanics site (left middle), first year ice next to the ridge observatory site (thickness 1.2 m, right middle), as well as first year ice (thickness 1.23 m) at the coring site (right). Site locations are depicted in Figure 1, except the first year ice coring site which lies about 2 km away.

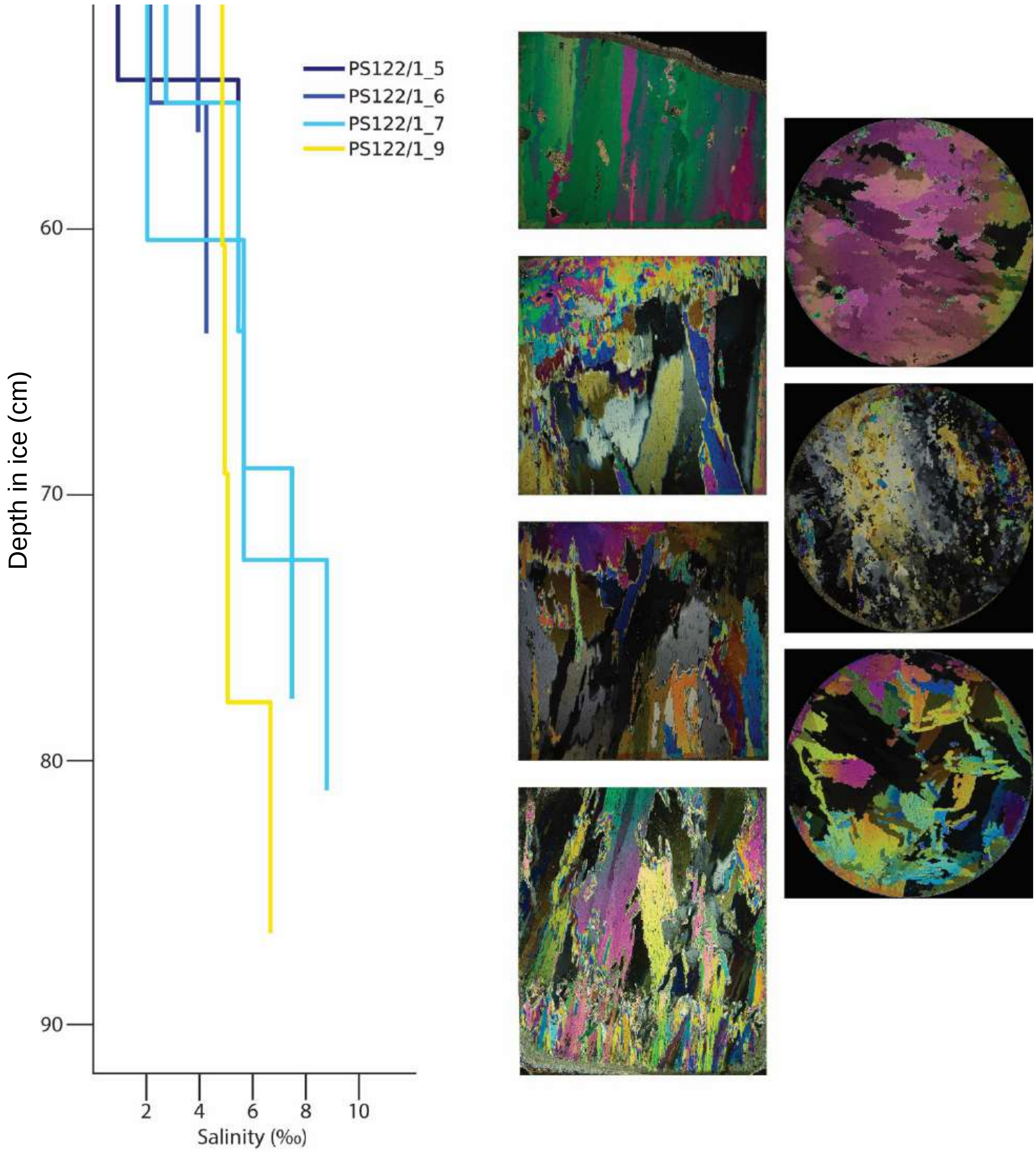

Figure S11. Bulk salinity of co-located ice cores (left) and ice stratigraphy of the lower 30 cm of an ice core collected at the second-year ice site on 25 November (PS122/1_9) before platelet ice was observed by the ROV. Vertical (rectangular) and horizontal (circular) thin sections photographed between crossed polarizers. The upper part of the core (not shown), from the surface down to about 55 cm depth, consists of remnant sea ice from the previous year. The three lower vertical sections of the ice core, starting at roughly 63 cm depth, exhibit strongly misaligned, platy crystals characteristic of platelet ice, differing substantially from columnar ice.

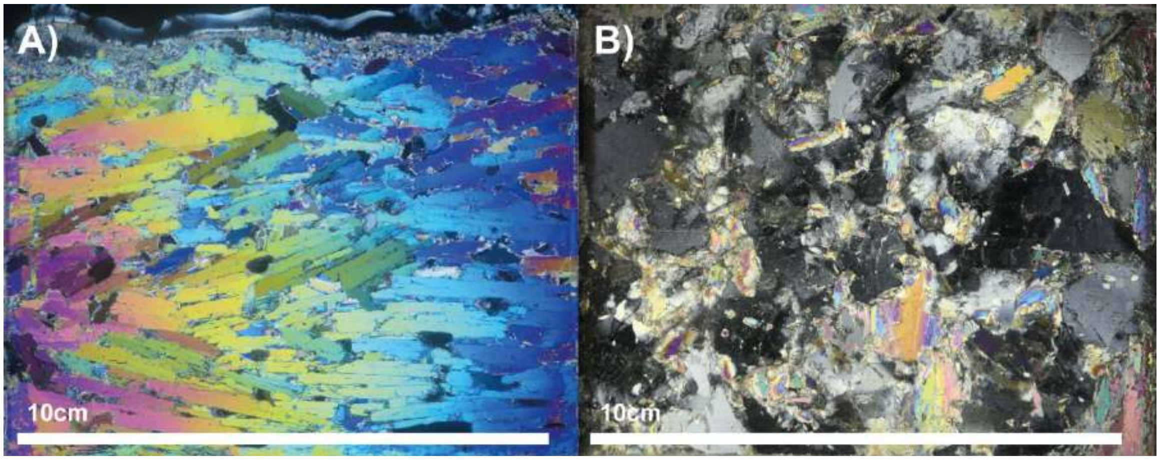

Figure S12. Thin sections of ice platelets collected with the ROVnet and refrozen with seawater in a styrofoam box photographed under crossed polarizers: A) vertical thin section showing individual platelets from the side. B) horizontal thin section showing that c-axis orientation is mostly normal to the platelet.

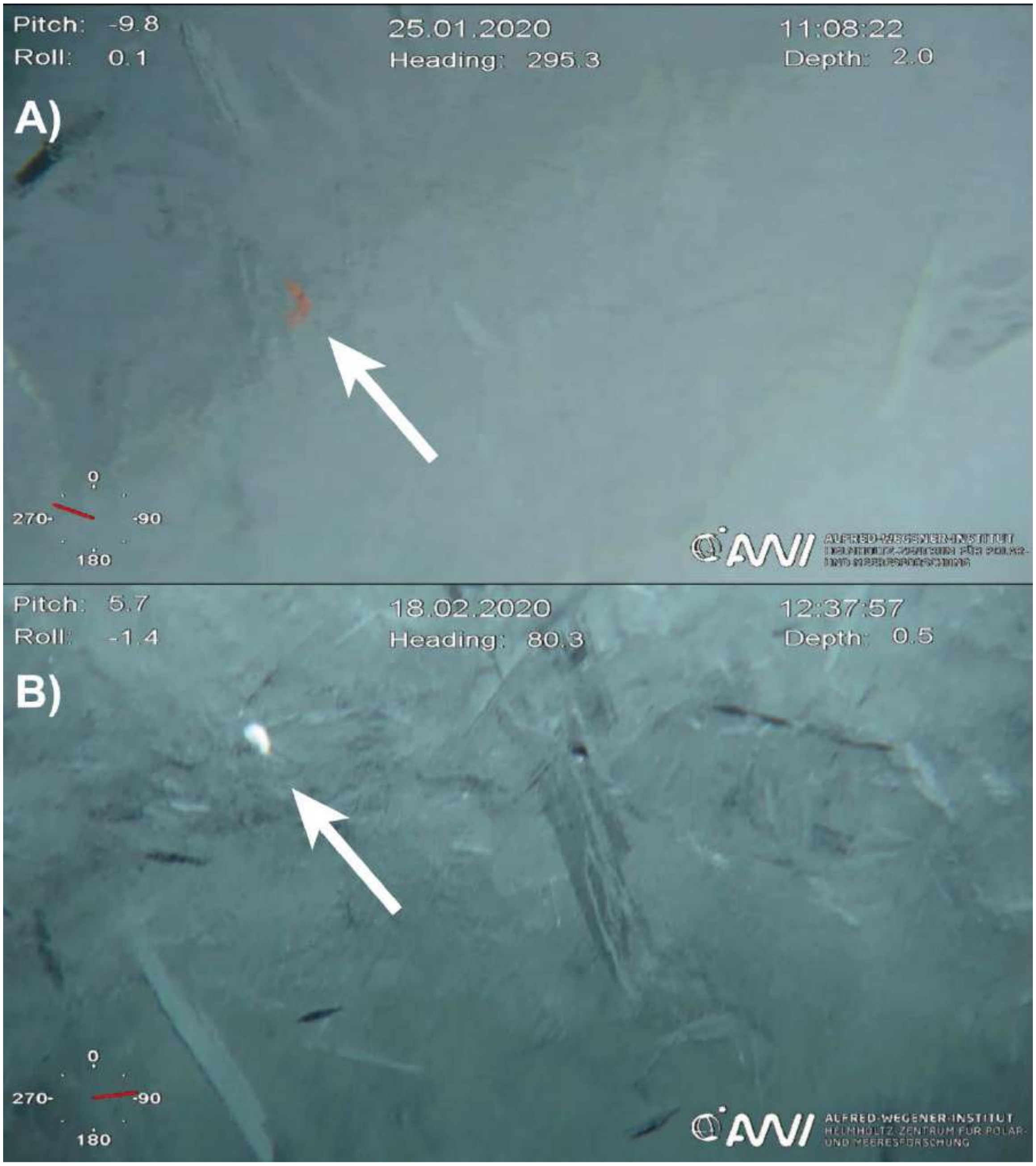

Figure S13. A&B) Under-ice macro fauna – probably amphipods – roaming in between the ice platelets.

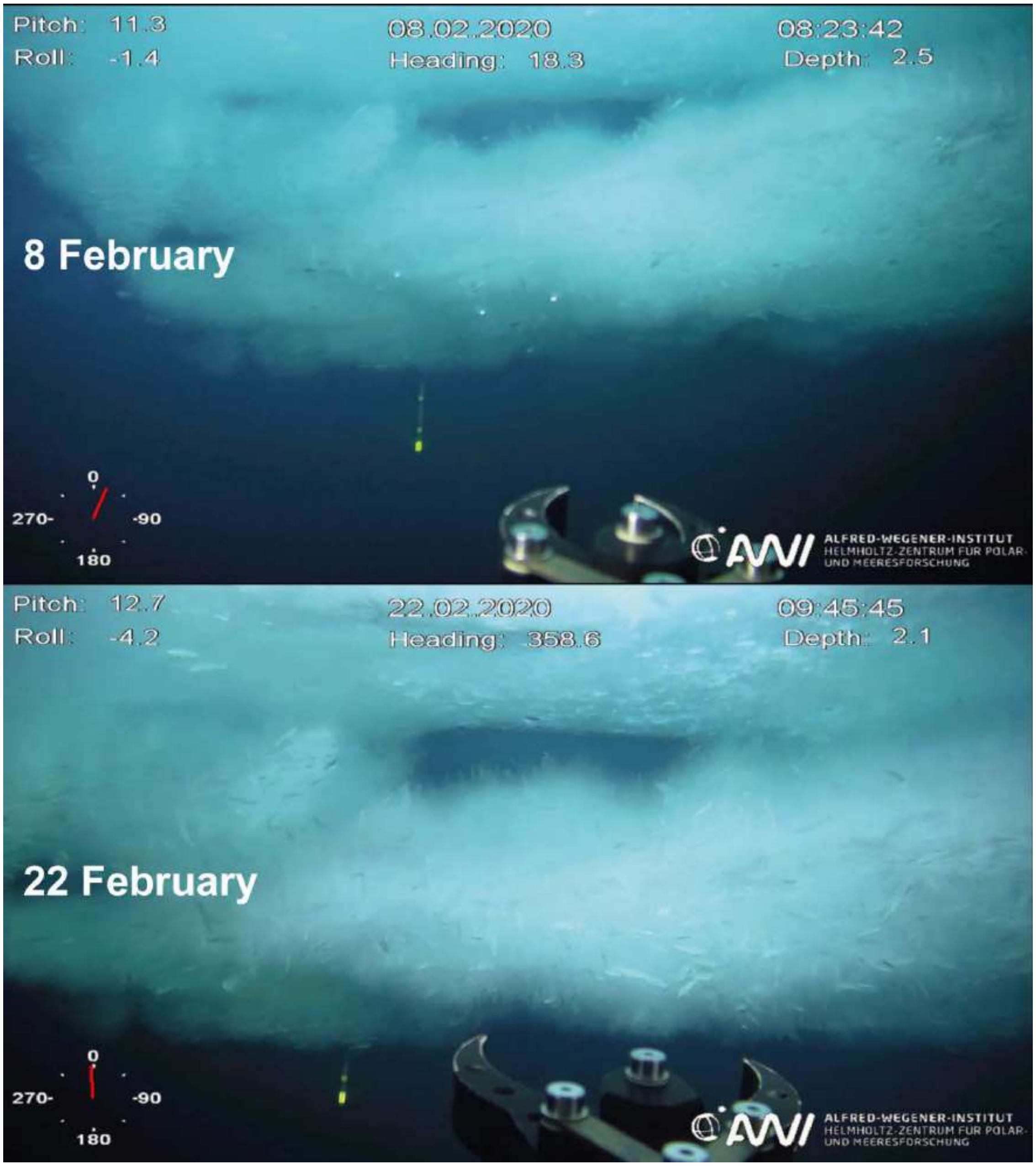

Figure S14. Time series of under-ice photographs showing the development of "upward-growing" platelet ice on top of a rafted floe.

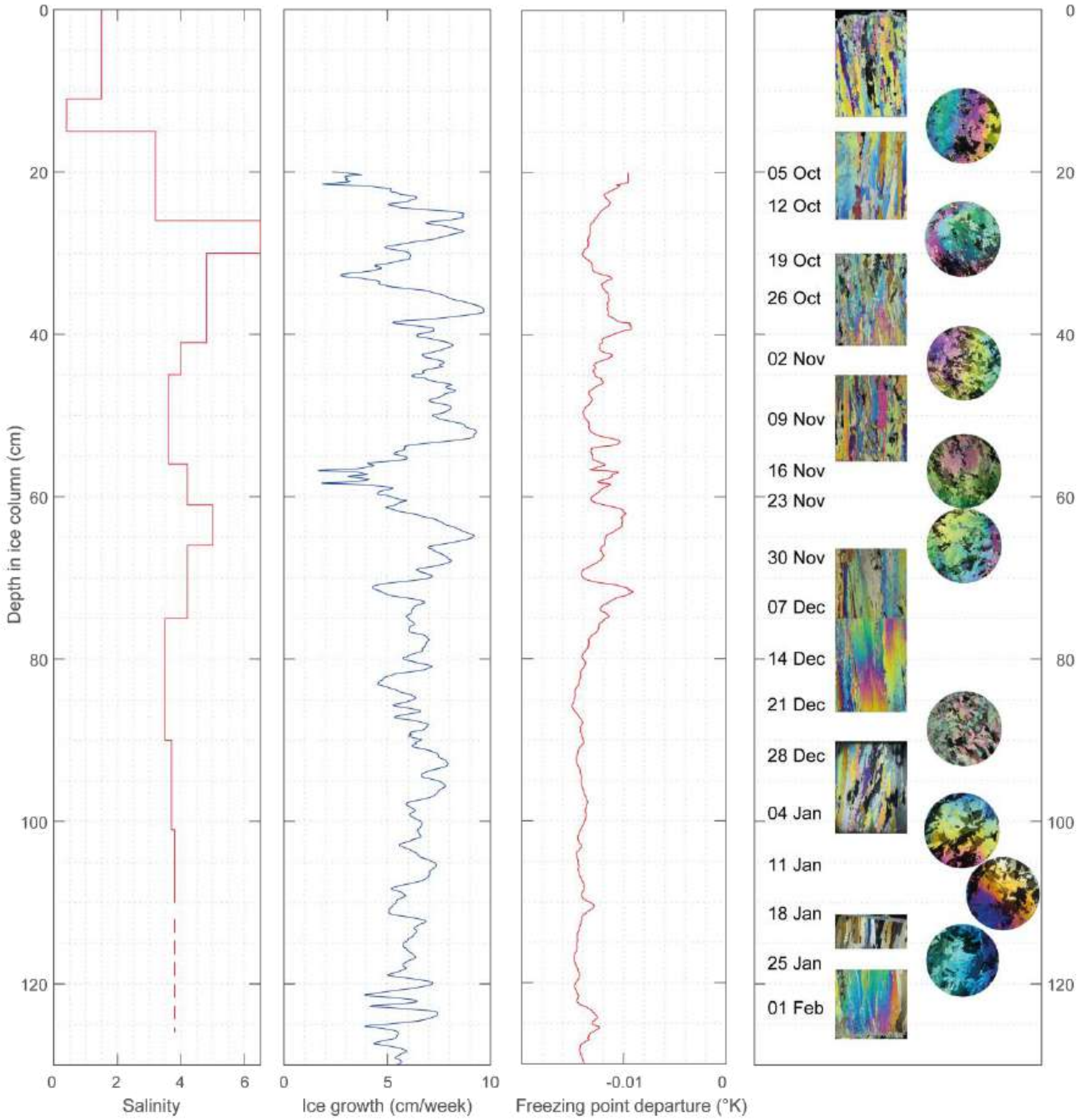

Figure S15. Analysis of the ice core retrieved on level first year ice / residual ice in the ROV survey area next to the ridge observatory. Bulk salinity (left), ice growth derived from a thermodynamic model (left middle), time-coincident freezing point departure as derived from autonomous buoy O4 (right middle). Vertical (rectangular) and horizontal (circular) thin sections along with ice formation date according to the thermodynamic model (right).

References:

Bardout, G., E. Périé, and B. Poyelle (2011), On a marché sous le pôle : Deepsea under the Pole, Chêne, [Paris].

Carnat, G., T. Papakyriakou, N. X. Geilfus, F. Brabant, B. Delille, M. Vancoppenolle, G. Gilson, J. Zhou, and J.-L. Tison (2017), Investigations on physical and textural properties of Arctic first-year sea ice in the Amundsen Gulf, Canada, November 2007–June 2008 (IPY-CFL system study), J. Glaciol., 59(217), 819-837, doi:10.3189/2013JoG12J148.

Jeffries, M. O., K. Schwartz, K. Morris, A. D. Veazey, H. R. Krouse, and S. Gushing (1995), Evidence for platelet ice accretion in Arctic sea ice development, Journal of Geophysical Research: Oceans, 100(C6), 10905-10914, doi:10.1029/95jc00804.

Kirillov, S., I. Dmitrenko, S. Rysgaard, D. Babb, J. Ehn, J. Bendtsen, W. Boone, D. Barber, and N. Geilfus (2018), The Inferred Formation of a Subice Platelet Layer Below the Multiyear Landfast Sea Ice in the Wandel Sea (NE Greenland) Induced by Meltwater Drainage, Journal of Geophysical Research: Oceans, 123(5), 3489-3506, doi:10.1029/2017jc013672.

Lewis, E. L., and A. R. Milne (1977), Underwater sea ice formation in "Polar Oceans," paper presented at Proc. SCOR/SCAR Polar Oceans Conference, Arctic Institute North America.

McDougall, T. J., and P. M. Barker (2011), Getting started with TEOS-10 and the Gibbs Seawater (GSW) Oceanographic Toolbox, Trevor J McDougall, Battery Point, Tas.

Ragobert, T., et al. (2008), Tara : journey to the heart of the climate machine, edited.